9

Implications of the MSSM

In this chapter, we discuss various implications of the MSSM relevant to low energy experiments in particle physics and to cosmology. We will postpone examination of signals from direct production of sparticles at high energy colliders to later chapters.

In any theory (like the MSSM) with many scalar fields, there are potentially new sources of flavor-changing neutral currents (FCNC). Experiment tells us that such flavor-violating effects are strongly suppressed. Experimental constraints on these restrict the form of soft SUSY breaking masses and couplings in the MSSM. As we will discuss in more detail, viable models may be classified by the pattern (universality, alignment or decoupling) of scalar mass matrices. We also discuss constraints from potentially large CP-violating processes such as the electric dipole moment of the electron and neutron.

We then proceed to study the effects of renormalization in the MSSM, which differ from corresponding effects in the SM because of the presence of weak scale superpartners. The prediction of gauge coupling unification in the MSSM – but not in the SM – is the best known, and perhaps the most spectacular, of these differences. It is possible to view the MSSM as a theory *defined* at the scale $M_{\rm SUSY} \sim M_{\rm weak}$, but with > 100 additional parameters that have well-defined values at that scale. However, since the MSSM is stable against radiative corrections, it may be valid up to much larger energy scales, perhaps as high as those associated with grand unification or string phenomena. New physics at these scales may provide an organizing principle that determines the multitude of weak scale SUSY parameters in terms of a few more fundamental parameters. The renormalization group equations (RGEs) then provide a link between the parameters of the theory at these ultra-high energy scales, and the weak scale, where superpartners are expected to be observed. In particular, we show that the breakdown of electroweak symmetry may be a *derived* consequence of the breakdown of supersymmetry, resulting from the large top quark Yukawa coupling. This picture fits in neatly with the recent discovery of the top quark with $m_t \simeq 175$ GeV. To avoid fine-tuning of SUSY

https://doi.org/10.1017/9781009289801.010 Published online by Cambridge University Press

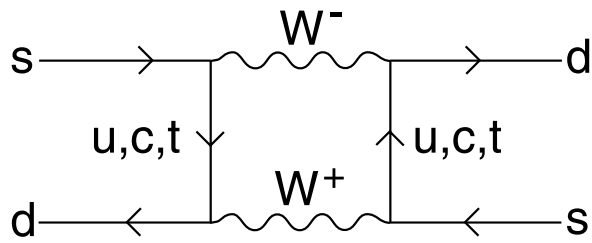

Figure 9.1 A SM box diagram contributing to the K_L–K_S mass difference.

parameters associated with electroweak symmetry breaking, a "naturalness" constraint suggests that SUSY particles that couple directly to the Higgs sector ought to have masses below ∼1 TeV, and hence ought to be accessible to collider search experiments in the near future.

Having set up the framework, we proceed to quantify how various observations restrict the values of the soft SUSY breaking masses in the MSSM. These include measurements of the rare decays $b \to s\gamma$ and $B_s \to \mu^+\mu^-$, the anomalous magnetic moment $a_\mu = (g-2)_\mu/2$ of the muon, and determination of the amount of relic neutralino "dark matter" left over from the Big Bang. If R-parity is indeed conserved (as we assume in the MSSM), then the lightest supersymmetric particle (LSP) should be absolutely stable, and LSPs produced in the early Universe should pervade all space, and could form the bulk of the dark matter that is required to exist by astrophysical measurements. If these cosmological relics are gravitationally clumped in our galactic halo, they may be detectable by both direct and indirect dark matter search experiments.

9.1 Low energy constraints on the MSSM

9.1.1 The SUSY flavor problem

Flavor-changing neutral current processes are forbidden at tree level in the SM due to the GIM mechanism. However, non-zero FCNC rates do occur in the SM at the loop level. A famous example occurs in the neutral K-meson system, where the $K_L - K_S$ mass difference can be calculated from box diagrams such as the one listed in Fig. 9.1. The contribution from the charm quark dominates, and the SM contribution to Δm_K is approximately given by

$$\Delta m_K \simeq \frac{G_F}{\sqrt{2}}\frac{\alpha}{6\pi}\frac{f_K^2 m_K}{\sin^2\theta_W}\cos^2\theta_C \sin^2\theta_C \frac{m_c^2}{M_W^2}, \tag{9.1}$$

where f_K is the kaon decay constant, θ_C is the Cabibbo mixing angle, and m_c is the charm quark mass. The kaon mass difference was, in fact, used to predict the charm quark mass shortly before the discovery of charm.

https://doi.org/10.1017/9781009289801.010 Published online by Cambridge University Press

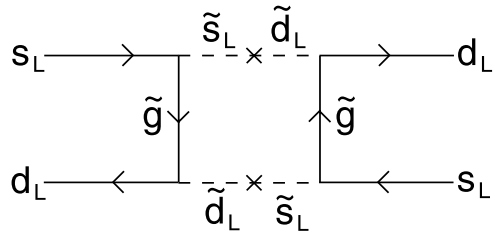

Figure 9.2 An MSSM box diagram contributing to the K_L–K_S mass difference.

In the MSSM, additional contributions from box diagrams involving squarks and gluinos are also present, such as the one shown in Fig. 9.2. (Other diagrams involving chargino and neutralino loops also contribute.) The cross in Fig. 9.2 represents an off-diagonal entry in the squark mass squared matrix

$$\mathcal{L}_{\text{soft}} \ni \tilde{d}_L^\dagger (\mathbf{m}_Q^2)_{12} \tilde{s}_L,$$

which naively is expected to be comparable to the corresponding diagonal entry: 100–1000 GeV. In this case, SUSY contributions to Δm_K violate limits from experiment, and the model is excluded. This is an example of what is referred to as the *SUSY flavor problem*. It occurs because the transformation that diagonalizes the quark mass matrices does not simultaneously diagonalize the corresponding squark mass squared matrices. It is up to theorists to devise models that restrict soft SUSY breaking mass matrices in such a way that bounds from FCNC processes are not violated.

Diagonalization of scalar mass matrices is always possible, but the large off-diagonal mass matrix elements will then lead to non-degenerate squarks that *all* couple via the gluino to *both* s and d quarks. If U denotes the unitary matrix that diagonalizes the quark mass matrix, and $\tilde{U}$ the unitary matrix that diagonalizes the squark mass matrix, the $\tilde{g} - \tilde{q} - q$ interaction (in the mass basis for quarks and squarks) will be proportional to $U\tilde{U}^\dagger$. A calculation of the complete box diagram shows that the contribution to Δm_K is proportional to

$$\sum_{\alpha,\beta=\tilde{d}_L,\tilde{s}_L,\tilde{b}_L} (U\tilde{U}^\dagger)_{i\alpha}(U\tilde{U}^\dagger)^*_{j\alpha}(U\tilde{U}^\dagger)_{i\beta}(U\tilde{U}^\dagger)^*_{j\beta} f(m_\alpha^2, m_\beta^2), \tag{9.2}$$

where i and j label the external quarks, α and β label the internal squarks, and f is some function of the left-squark mass eigenvalues. A necessary condition for flavor-changing processes is that there are large off-diagonal entries in the $U\tilde{U}^\dagger$ matrix.

Exercise *Convince yourself that if the left-squark mass matrix has degenerate eigenvalues so that $f(m_\alpha^2, m_\beta^2)$ is independent of the squark indices, the gluino*

https://doi.org/10.1017/9781009289801.010 Published online by Cambridge University Press

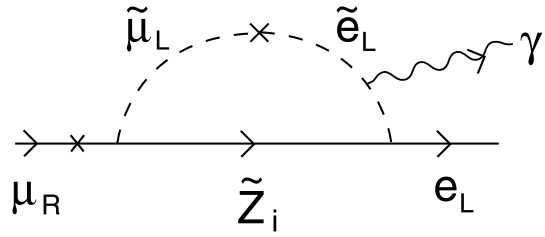

Figure 9.3 Feynman diagram contributing to $\mu \to e\gamma$ decay via a SUSY loop.

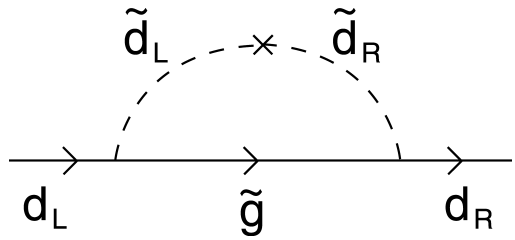

Figure 9.4 An MSSM contribution to the down quark self-energy.

contribution to Δm_K vanishes. The same argument clearly holds for the neutralino contribution. Work out the corresponding argument for chargino contributions.

Flavor violation is not confined to the kaons. A large off-diagonal entry $(\mathbf{m}_Q^2)_{23}$ or $(\mathbf{m}_D^2)_{23}$ (or worse, $(\mathbf{a_d})_{23}$, discussed below) would result in large flavor-violating gluino vertices, and an unacceptable rate for $b \to s\gamma$ decays via diagrams involving squark and gluino loops, analogous to those in Fig. 9.3 with (s)leptons replaced by s(quarks) and the neutralino by the gluino, or in Fig. 9.4 with a photon attached to the squark line.

Eq. (9.2) then suggests three distinct mechanisms to avoid large FCNCs in the MSSM, and thus to solve the SUSY flavor problem. The first two suppress the off-diagonal entries in (9.2) while the third suppresses loop effects by making sparticles very heavy.

1. Arrange for *degeneracy* amongst the masses of squarks with the same quantum numbers.
2. Arrange the SUSY breaking mechanism so that squark and quark mass matrices are diagonalized by the same unitary transformation, so that the matrix $U\tilde{U}^\dagger \simeq \mathbf{1}$. Squarks can be non-degenerate. In this case, the quark and squark mass matrices are said to be *aligned*.[1] Such an alignment can be arranged in models which include so-called *horizontal* symmetries, linking the various generations.

[1] Y. Nir and N. Seiberg, *Phys. Lett.* **B309**, 337 (1993).

https://doi.org/10.1017/9781009289801.010 Published online by Cambridge University Press

3. The third method to suppress FCNCs is to simply assume that the masses of the squarks circulating in the box diagrams are so heavy that the diagram is suppressed. This solution to the SUSY flavor problem is known as *decoupling*. Detailed computations of the K_L–K_S mass difference including QCD corrections indicate that first and second generation squark masses should be larger than $\sim$ 40 TeV to adequately suppress FCNCs. At first sight, this seemingly contradicts *naturalness* constraints that imply superpartner masses should lie at or below the TeV scale. We should note though that these apply most directly to sparticles that have substantial couplings to the Higgs boson sector, i.e. to charginos and neutralinos and third generation sfermions. The first two generations of sfermions which couple to Higgs bosons only via tiny Yukawa couplings or indirectly at the two-loop level may be considerably more massive.

Additional constraints on squark masses and mixing matrices come from measurements of B-$\overline{B}$ and D-$\overline{D}$ mass differences, and from lepton sector FCNC processes such as $\mu \to e\gamma$ (an example is given in Fig. 9.3), $\tau \to \mu\gamma$, and $\tau \to e\gamma$.[2] The constraints that can be extracted vary in their severity, but all can be fulfilled by implementing one or a combination of the solutions of degeneracy, alignment or decoupling.

Constraints from FCNCs also restrict the form of the soft SUSY breaking trilinear terms $(\mathbf{a}_u)_{ij}$, $(\mathbf{a}_d)_{ij}$, and $(\mathbf{a}_e)_{ij}$. For instance, when a Higgs field develops a VEV, then off-diagonal mass terms such as

$$(\mathbf{a}_d)_{12}\tilde{Q}_1^a H_{da}\tilde{d}_{R2}^\dagger \to (\mathbf{a}_d)_{12} v_d \tilde{d}_L \tilde{s}_R^\dagger \tag{9.3a}$$

or flavor-diagonal masses such as

$$(\mathbf{a}_d)_{11}\tilde{Q}_1^a H_{da}\tilde{d}_{R1}^\dagger \to (\mathbf{a}_d)_{11} v_d \tilde{d}_L \tilde{d}_R^\dagger \tag{9.3b}$$

will be induced. The first of these will again be restricted by processes such as K–$\overline{K}$ mixing, so that we must require the off-diagonal entries of the $\mathbf{a}$ matrix to be small. The second of these terms can make (flavor-conserving) contributions to *fermion* masses, such as the down quark via gluino–squark loops (see Fig. 9.4). Requiring these contributions to fermion masses to be smaller (in order of magnitude) than the fermion masses themselves leads to tight constraints on the magnitudes of terms such as $(\mathbf{a}_u)_{ii}$ and $(\mathbf{a}_d)_{ii}$ and $(\mathbf{a}_e)_{ii}$, for generations $i = 1$ and 2.

[2] For a general analysis of FCNC and CP-violating effects, see F. Gabbiani, E. Gabrielli, A. Masiero and L. Silvestrini, *Nucl. Phys.* **B477**, 321 (1996).

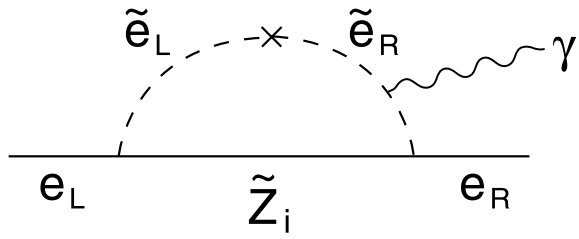

Figure 9.5 A supersymmetric contribution to the electric dipole moment of the electron.

9.1.2 The SUSY CP violation problem

Since, as discussed in Chapter 8, soft SUSY breaking parameters are in general complex, one should expect TeV scale imaginary components to these, which would correspond to the presence of large CP-violating phases. Many constraints on these imaginary components can also be extracted from low energy data. For instance, SUSY contributions to the parameter $\epsilon_K = \frac{1}{2}\frac{\mathrm{Im}\langle K|\mathcal{H}_{eff}|\overline{K}\rangle}{\mathrm{Re}\langle K|\mathcal{H}_{eff}|\overline{K}\rangle}$ can be used to set bounds on the *imaginary* part of squark mass squared matrix elements. The flavor-violating contributions have been parametrized by Gabbiani *et al.* as complex "mass insertions" $(\Delta m^2)^{ab}_{ij}$ (i, j label the flavor and a, b = L, R the squark type), and the constraints are expressed as bounds on dimensionless quantities $\delta^{ab}_{ij} = (\Delta m^2)^{ab}_{ij}/\tilde{m}^2$. Measurements of Δm_K and ϵ_K put constraints on the δ^{ab}_{12}, but further assumptions are needed to extract these. For instance, assuming that the real parts of the δs dominate their imaginary parts, and further that the real part is at its upper bound, one can obtain an upper limit on the imaginary part. As an example: for $m_{\tilde{q}} \sim m_{\tilde{g}} = \tilde{m}$, the general analysis from Gabbiani *et al.* shows that for the down squark sector, $\sqrt{\mathrm{Im}(\Delta m^2)^{LL}_{12}} \leq 0.01\tilde{m}$.

Limits on the imaginary parts of the soft SUSY breaking **a** terms can be obtained from experimental upper limits on the electric dipole moments (EDMs) of both the electron and the neutron. These contributions come from diagrams such as those depicted in Fig. 9.5. For instance, the quantity $\sqrt{|\mathrm{Im}(\mathbf{a}_e)_{11} v_d|}$ is restricted to be less than $6 \times 10^{-4} m_{\tilde{e}}$. Likewise, the bound on the neutron electric dipole moment restricts $\sqrt{|\mathrm{Im}(\mathbf{a}_d)_{11} v_d|}$ to be less than $\sim 0.002 m_{\tilde{d}}$. In the case of R-parity-violating scenarios, phases of R-parity-violating couplings are also restricted by similar considerations.

Finally, measurements of the CP-violating decays $K_L \to \pi\pi$ are related to the CP-violating parameter ϵ'_K. These measurements further restrict $\sqrt{|\mathrm{Im}(\mathbf{a}_d)_{12} v_d|}$ to be smaller than $\sim 0.004 m_{\tilde{d}}$.

Determining the physical principle behind why so many of the CP-violating phases are so small is known as the *SUSY CP problem*. Motivated by the stringent limits on the magnitude of CP-violating phases, an ad hoc but frequent assumption

https://doi.org/10.1017/9781009289801.010 Published online by Cambridge University Press

in the literature is to simply ignore them, and set all the imaginary parts of soft SUSY breaking parameters as well as μ to zero. This is not meant to be taken literally. In many analyses not involving CP violation (e.g. direct searches for sparticles), these *small* phases make little difference. An alternative solution is to again assume the SUSY particles circulating in the loops are so heavy – in the multi-TeV range – that the CP-violating contributions are suppressed. SUSY model builders, however, have to explain why SUSY contributions to CP violation are small, and perhaps to make predictions for the patterns of CP violation for the third generation where data are not yet in.

A common but stronger assumption which solves both the SUSY flavor and CP problems is to assume *universality* and *reality* of soft SUSY breaking masses:

$$\mathbf{m}_Q^2 = m_Q^2\mathbf{1};\ \ \mathbf{m}_U^2 = m_U^2\mathbf{1};\ \ \mathbf{m}_D^2 = m_D^2\mathbf{1};\ \ \mathbf{m}_{\rm L}^2 = m_{\rm L}^2\mathbf{1};\ \ \mathbf{m}_E^2 = m_E^2\mathbf{1}. \tag{9.4}$$

In addition, the trilinear **a** terms are assumed proportional to their corresponding Yukawa matrices:

$$\mathbf{a}_u = A_u\mathbf{f}_u;\ \ \mathbf{a}_d = A_d\mathbf{f}_d;\ \ \mathbf{a}_e = A_e\mathbf{f}_e. \tag{9.5}$$

In this case, almost all FCNC contributions will be well below experimental limits (a super-GIM mechanism operates), and all CP-violating phases other than in the usual CKM mixing matrix will be vanishing. The universality assumption, however, goes beyond just fulfilling experimental constraints. In particular, it should be kept in mind that restrictions on many of the soft SUSY breaking mass parameters are very loose or even non-existent, and it remains for experimental measurements to determine or limit these parameters.

9.1.3 Large CP-violating parameters in the MSSM?

As we have discussed, measurements of the EDM of the electron and the neutron and, most recently, of atoms such as mercury have placed stringent constraints on CP-violating phenomena in the MSSM. However, these constraints do *not* guarantee that many of the CP-violating MSSM parameters are small. It could be that flavor-blind CP-violating parameters (such as the gaugino masses M_i') and CP-violating phases associated with the first two generations are small, but those associated with the third generation are large. Or, it could be that sparticle masses are in the multi-TeV range so that SUSY loop contributions to the various EDMs are suppressed even if the CP-violating parameters are relatively large. Finally, it could be that individual phases/parameters are large, but that there exist cancellations amongst the amplitudes which contribute to the various EDMs. Any theory of SUSY breaking would then have to explain the origin of these cancellations if they

https://doi.org/10.1017/9781009289801.010 Published online by Cambridge University Press

are not to be attributed to mere accident. We caution the reader that there is no clear consensus in the literature as to just how well these cancellation mechanisms work. In part, this is because the conversion of the stringent experimental bound on the EDM of mercury to limits on the EDM of quarks and electrons (or its QCD analogue, the chromo electric dipole moment of quarks) that are predicted by any high scale theory is not entirely straightforward. A careful assessment of the associated subtleties is beyond the scope of this text, and we refer the interested reader to the literature for a discussion of these issues.[3]

If indeed the CP-violating parameters are large, these can lead to observable effects in the sparticle and Higgs boson sectors, even in non-CP-violating phenomena. One simple example comes from the chargino mass matrix, exemplified in the exercise at the end of this section. In Chapter 8, we noted that while one of the CP-violating phases associated with gaugino masses (we chose the case of M_3') could be rotated away, the remaining two could not. Thus, M_2' and also a complex phase in the μ parameter (where $\mu = |\mu|e^{i\phi_\mu}$) would enter the chargino mass matrix and alter the corresponding physical chargino mass eigenvalues. The CP-violating parameters would also modify the chargino mixing matrices, and hence could modify chargino production cross sections and branching fractions. Likewise, neutralino mass eigenvalues, production rates, and decay rates can depend on M_1', M_2', and ϕ_μ. Squark and slepton observables can depend on these parameters, as well as on possibly large CP-violating phases in the **a**-parameters: within the mSUGRA-like framework with a universal A-parameter introduced in Section 9.2.2, this effect is most pronounced for the third generation sfermions. If SUSY sources of CP violation are large, Higgs boson phenomenology may also be significantly altered: in particular, as already alluded to in Section 8.3.3, neutral Higgs bosons would no longer be mass eigenstates, and their phenomenology would be correspondingly altered. These new sources of CP violation can also obviously lead to novel effects in the physics of K and B mesons, since not all CP-violating effects would then be described by the Kobayashi–Maskawa phase.[4] These SUSY sources of CP violation may also have a significant impact on cosmology at early times, most notably on baryogenesis.

[3] The EDM of mercury was evaluated within the MSSM framework by T. Falk, K. Olive, M. Pospelov and R. Roiban, *Nucl. Phys.* **B560**, 3 (1999). For an overview of the potential uncertainties in this evaluation, see e.g. the reviews by Ibrahim and P. Nath, hep-ph/0210251 (2002) and D. Chung *et al.*, hep-ph/0312378 (2003), and references cited therein. An overview of how SUSY CP violation affects sparticle phenomenology is also contained in these reviews. See also, J. Erler and M. Ramsey-Musolf, hep-ph/0404291 for a general discussion of the evaluation of EDMs within extensions of the SM.

[4] For instance, determination of the angles of the so-called unitarity triangles in different processes will not yield consistent values for these. Especially topical at the time of this writing is the discrepancy in the decays $B \to \phi K_s$ vis-à-vis the decays $B \to \psi K_s$, reported by the BELLE experiment. This discrepancy has, however, not been seen by the BaBar experiment. For textbook discussions of these questions see G. Branco, L. Lavoura and J. Silva, *CP Violation*, Oxford (1999); I. Bigi and A. Sanda, *CP Violation*, Cambridge University Press (2000).

We will for simplicity of discussion ignore the possibility of large CP-violating parameters in the remainder of this book. We expect that the interested reader will be able to carry out the necessary modifications to include their effects in the discussion.

Exercise *To illustrate the potential impact of CP-violating SUSY parameters on sparticle masses and couplings, generalize the derivation of the chargino masses and mixing patterns in Section 8.3.5 to the case where the CP-violating gaugino mass term M_2' does not vanish, and the supersymmetric parameter μ is complex.*

Working in the convention that the Higgs scalars have real VEVs (this may lead to CP-violating phases in the interactions of Higgs bosons with other scalars) show that the mass terms for the charginos can now be written as,

$$\mathcal{L}_{\text{chargino}} = -\left(\bar{\lambda},\ \bar{\tilde{\chi}}\right)\left(\mathcal{M}_{\text{charge}} P_{\text{L}} + \mathcal{M}^{\dagger}_{\text{charge}} P_{\text{R}}\right)\begin{pmatrix}\lambda\\ \tilde{\chi}\end{pmatrix},$$

where now

$$\mathcal{M}_{\text{charge}} = \begin{pmatrix} M_2 - \mathrm{i}M_2' & -g v_d \\ -g v_u & -\mu \end{pmatrix}.$$

Many authors who use the two-component notation introduce instead a complex mass $\mathcal{M}_2 \equiv M_2 - \mathrm{i}M_2'$ and write $\mathcal{M}_2 \equiv |\mathcal{M}_2| \mathrm{e}^{\mathrm{i}\phi_2}$, and work with the real numbers $|\mathcal{M}_2|$ and ϕ_2 instead of our M_2 and M_2', as alluded to at the very end of Chapter 7.

Show that the squared chargino masses, the eigenvalues of the matrix $\mathcal{M}_{\text{charge}}\mathcal{M}^{\dagger}_{\text{charge}}$, are now given by,

$$m^2_{\widetilde{W}_{1,2}} = \frac{1}{2}\left[(|\mu|^2 + |\mathcal{M}_2|^2 + 2M_W^2) \mp \zeta\right],$$

with

$$\zeta^2 = (|\mu|^2 - |\mathcal{M}_2|^2)^2 + 4M_W^2\big[M_W^2 \cos^2 2\beta + |\mu|^2 + |\mathcal{M}_2|^2 \\ -2|\mu||\mathcal{M}_2| \sin 2\beta \cos(\phi_\mu + \phi_2)\big].$$

Notice that if $|\mathcal{M}_2| = \sqrt{M_2^2 + M_2'^2}$ and/or $|\mu|$ are much larger than M_W, once again the two charginos are dominantly gauginos and higgsinos.

The matrices U and V that enter the chargino couplings via the diagonalization of charginos (see Sec. 8.3.5) will now depend on these additional CP-violating parameters, and potentially cause CP violation in processes involving charginos.

The effect of CP-violating gaugino masses and complex μ term on the neutralino sector can be similarly worked out.

---

https://doi.org/10.1017/9781009289801.010 Published online by Cambridge University Press

9.2 Renormalization group equations

Since the MSSM is free of quadratic divergences, mass parameters of order the weak scale remain stable under radiative corrections. In particular, if the MSSM is embedded in a larger framework, such as a GUT or string model, parameters of order the weak scale will remain that same order even after radiative corrections involving the ultra-high energy scales associated with these models. This stabilization of mass hierarchies allows the possibility of reliably extending the predictions of the MSSM up to very high energy scales. Logarithmic divergences, however, remain, and perturbative calculations involving energies $Q \sim M_{\rm GUT}$ will typically contain powers of $\frac{\alpha_i}{4\pi}\log(M_{\rm GUT}/M_Z)$, where α_i is a gauge coupling. Fortunately, these large logarithms which would invalidate the perturbative expansion in α_i can be summed by using renormalization group methods. The coupling constants and mass parameters of the theory are replaced by running couplings and masses, with values depending on the energy scale. The scale dependence of the parameters of the theory is given by the renormalization group equations.

9.2.1 Gauge couplings and unification

In quantum field theory, perturbative calculations beyond tree level are usually performed using *renormalized perturbation theory* (RPT), as opposed to bare perturbation theory. The bare fields, mass terms and coupling constants that occur in the original Lagrangian are (perturbatively) divergent quantities. In RPT, these are replaced by finite, renormalized fields, masses and coupling constants, and divergent quantities are formally shuffled into *counterterms*. The form of the counterterms is determined by specifying renormalization conditions at some arbitrarily chosen energy scale Q, referred to as the renormalization scale. While Green functions of the bare theory are independent of the renormalization scale, Green functions calculated in RPT are dependent on the renormalization scale. The dependence of Green functions of RPT on shifts in the renormalization scale Q is governed by the Callan–Symanzik equation. As the renormalization scale shifts, so too do the fields, coupling constants and masses of the theory. The evolution of a coupling constant g with renormalization scale, in particular, is governed by the Callan–Symanzik beta function $\beta(g)$, defined as

$$\beta(g) = Q\frac{\partial g}{\partial Q}.$$

The procedure for evaluating β is to calculate the logarithmically divergent parts of diagrams which contribute to the coupling constant renormalization, and then take the logarithmic derivative with respect to the renormalization scale Q. For non-supersymmetric non-Abelian gauge theories, the calculation of the one-loop

https://doi.org/10.1017/9781009289801.010 Published online by Cambridge University Press

β-function is performed in many texts.[5] The result, generalized to include scalars and left- and right-handed fermions in different representations, is

$$\beta(g) = -\frac{g^3}{16\pi^2}\left[\frac{11}{3}C(G) - \frac{2}{3}n_{\rm F}S(R_{\rm F}) - \frac{1}{3}n_{\rm H}S(R_{\rm H})\right], \tag{9.6}$$

where $C(G)$ is the quadratic Casimir for the adjoint representation of the associated Lie algebra, $S(R_{\rm F})$ is the Dynkin index for representation $R_{\rm F}$ of the fermion fields, $S(R_{\rm H})$ is the Dynkin index for representation $R_{\rm H}$ of the scalar fields, $n_{\rm F}$ is the number of fermion species, and $n_{\rm H}$ is the number of complex scalars. For an $SU(N)$ gauge theory, for fermions or scalars in the fundamental N-dimensional representation, $S(R) = 1/2$, while $C(G) = N$. For small values of $n_{\rm F}$, the β-function is negative, resulting in the well-known phenomenon of asymptotic freedom.

For $SU(3)_{\rm C}$, with fermions $u_{\rm L}$, $d_{\rm L}$, $u_{\rm R}$ and $d_{\rm R}$, $n_{\rm F} = 4n_{\rm g}$, where $n_{\rm g}$ is the number of generations. For $SU(2)_{\rm L}$, with three colors of left doublet quarks and a single left doublet of leptons, $n_{\rm F}$ is again $4n_{\rm g}$. Finally, for $U(1)_{\rm Y}$, $S(R) = 1$, and we simply sum over the squared hypercharges of a complete generation: $\sum(Y/2)^2 = 10/3$. The final result for the SM, at one-loop, is

$$\beta_i = \frac{g_i^3}{16\pi^2}b_i, \tag{9.7}$$

where the b_i ($i = 1, 2, 3$) are given by

$$\begin{pmatrix} b_1 \\ b_2 \\ b_3 \end{pmatrix} = \begin{pmatrix} 0 \\ -\frac{22}{3} \\ -11 \end{pmatrix} + n_{\rm g}\begin{pmatrix} \frac{4}{3} \\ \frac{4}{3} \\ \frac{4}{3} \end{pmatrix} + n_{\rm H}\begin{pmatrix} \frac{1}{10} \\ \frac{1}{6} \\ 0 \end{pmatrix}, \tag{9.8}$$

$n_{\rm g}$ is the number of generations, and $n_{\rm H}$ is the number of (complex) Higgs doublets ($n_{\rm H} = 1$ in the SM). The expression for b_1 holds for the evolution of the rescaled charge $g_1 = \sqrt{5/3}g'$ appropriate for a GUT model.

In the MSSM, there will be additional loop contributions to the various counterterms involving gauginos, matter scalars, Higgs scalars and higgsinos. To calculate the various loop diagrams, a suitable regularization scheme must be chosen. For SM calculations, dimensional regularization (DREG) is most frequently chosen, since it preserves gauge symmetry and hence the validity of Ward identities in loop calculations. In models with supersymmetry, DREG is usually not the regulator of choice, since it violates supersymmetry. The reason is that, by modifying the dimensionality of spacetime, one introduces a mismatch between the number of degrees of freedom in vector fields versus their supersymmetric counterpart gauginos.

[5] See, for instance, M. Peskin and D. V. Schroeder, *Introduction to Quantum Field Theory*, Chapter 16, Addison-Wesley (1995).

A modification of DREG known as dimensional reduction (DRED) also modifies the dimensionality of spacetime, but maintains four-vectors as four-component objects.[6] DRED thus preserves supersymmetry, at least for one-loop calculations. Calculations using DRED versus DREG differ only in the finite parts of one-loop diagrams, but differ even in the divergent parts of two-loop diagrams. Thus, the RGEs calculated via DREG or via DRED will be equivalent to one-loop order.

In the MSSM, the β-functions are modified by superpartner contributions from gauginos, higgsinos and matter scalars. These can be readily computed from (9.6). Using $S(R) = N$ for the adjoint representation in $SU(N)$, it is straightforward to show that the one-loop β-functions for the MSSM take the form,

$$\beta(g) = -\frac{g^3}{16\pi^2}\left[3C(G) - S(R)\right], \tag{9.9}$$

where the Dynkin index $S(R)$ is summed over all the matter and Higgs fields, and their superpartners, in the model. This then yields,

$$\begin{pmatrix} b_1 \\ b_2 \\ b_3 \end{pmatrix} = \begin{pmatrix} 0 \\ -6 \\ -9 \end{pmatrix} + n_{\rm g}\begin{pmatrix} 2 \\ 2 \\ 2 \end{pmatrix} + n_{\rm H}\begin{pmatrix} \frac{3}{10} \\ \frac{1}{2} \\ 0 \end{pmatrix}. \tag{9.10}$$

Exercise *Using Eq. (9.6) to obtain the contributions of the superpartner gauginos, higgsinos, and sfermions, verify that the gauge β-functions for the MSSM are indeed as given by (9.9) and (9.10).*

The RGEs for the gauge couplings can now be simply integrated. The constant of integration can be fixed using the experimentally measured value of the gauge coupling at some reference scale Q_0. We then find,

$$\frac{1}{g_i(Q)^2} - \frac{1}{g_i(Q_0)^2} = -\frac{b_i}{8\pi^2}\ln\left(\frac{Q}{Q_0}\right). \tag{9.11}$$

In Fig. 9.6, we show how the gauge couplings, given by Eq. (9.11), evolve with the scale choice Q. It is customary to plot the inverse of $\alpha_i = g_i^2/4\pi$, beginning with the values of α_1, α_2, and α_3 which are known to high precision at the value $Q = M_Z$. The evolution in the SM is shown in Fig. 9.6*a*. The three gauge coupling constants evolve in a generally convergent direction towards higher energy scales, becoming roughly the same at $Q \sim 10^{13}$–10^{17} GeV. In Fig. 9.6*b*, the case for the MSSM is shown. Remarkably, the three gauge couplings unify with impressive precision at $Q \simeq 2 \times 10^{16}$ GeV! In this case, we have evolved the gauge couplings according to

[6] W. Siegel, *Phys. Lett.* **B84**, 193 (1979).

https://doi.org/10.1017/9781009289801.010 Published online by Cambridge University Press

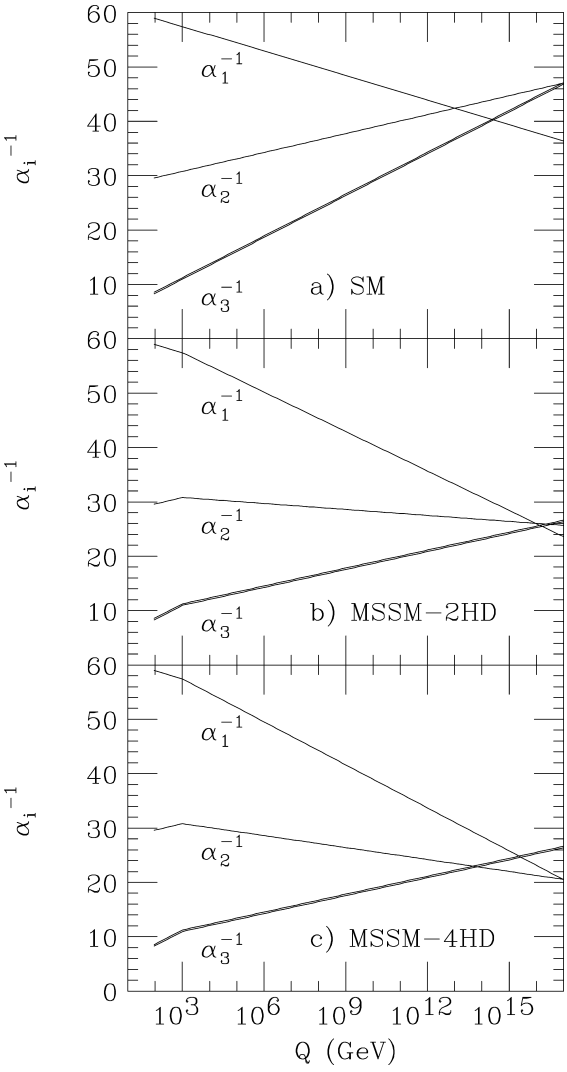

Figure 9.6 Evolution of the $SU(3)_C \times SU(2)_L \times U(1)_Y$ gauge coupling constants from the weak scale to the GUT scale for the case of (*a*) the SM, (*b*) the MSSM with two Higgs doublets, and (*c*) the MSSM with four Higgs doublets.

SM RGEs between $Q = 10^2$ and $Q = 10^3$ GeV, and switched to MSSM evolution equations for higher Q values. The gauge coupling unification in the MSSM is startling, and strongly suggests that the MSSM may be the remnant of some sort of supersymmetric grand unified theory, with superpartners around the TeV scale. In Fig. 9.6*c*, we show the same gauge coupling evolution, but this time we include four Higgs doublets in the supersymmetric model. For this case, gauge coupling unification is once again off the mark.

https://doi.org/10.1017/9781009289801.010 Published online by Cambridge University Press

The successful prediction of gauge coupling unification is viewed by many as indirect evidence for weak scale supersymmetry. It motivates us to consider the possibility that there may indeed be no new physics all the way up to a very high scale, and that the weakly coupled MSSM is valid up to $Q \sim M_{\rm GUT}$. This is an assumption. Above $Q = M_{\rm GUT}$, there may be new physics: gauge coupling unification suggests grand unification with a desert as the simplest possibility, but this need not be the case.

It is possible that an examination of the parameters of the MSSM renormalized at a very high scale (obtained from their measured values) might provide clues as to what this new physics might be, in the same way that the unification of gauge couplings points to grand unification. But such a bottom-up approach is clearly not possible today since we do not know the weak scale values of the SUSY parameters or even the superpotential Yukawa couplings. Instead, what is usually done is to make *simple* ansätze about the values of these soft SUSY breaking parameters at the high scale, and then evolve these down to the weak scale relevant for phenomenology using renormalization group equations. These ansätze serve as boundary conditions for the evolution.[7] It should be stressed that the evolution does not involve any new physics beyond the MSSM.

Typically, the simple boundary conditions can be expressed in terms of just a handful of parameters, from which all the parameters of the MSSM may be computed. In this sense, the MSSM augmented by the boundary conditions is a very predictive framework. As discussed in Chapter 7, we hope that an understanding of the physics of supersymmetry breaking, and its mediation to the observable sector, will yield the correct boundary conditions. In Chapter 11, we will discuss various models for SUSY breaking, but for the present we will regard the specification of the boundary values of the soft supersymmetry breaking parameters as an additional ansatz.

We have already studied the renormalization group equations for the gauge couplings. The one-loop RGEs for third generation Yukawa couplings of the MSSM are given by

$$\frac{\mathrm{d}f_t}{\mathrm{d}t} = \frac{f_t}{16\pi^2}\left(-\sum_{i=1-3} c_i g_i^2 + 6f_t^2 + f_b^2\right), \tag{9.12a}$$

$$\frac{\mathrm{d}f_b}{\mathrm{d}t} = \frac{f_b}{16\pi^2}\left(-\sum_{i=1-3} c_i' g_i^2 + f_t^2 + 6f_b^2 + f_\tau^2\right), \tag{9.12b}$$

$$\frac{\mathrm{d}f_\tau}{\mathrm{d}t} = \frac{f_\tau}{16\pi^2}\left(-\sum_{i=1-3} c_i'' g_i^2 + 3f_b^2 + 4f_\tau^2\right), \tag{9.12c}$$

[7] Of course, care must be taken to ensure that these boundary conditions lead to weak scale parameters consistent with all experimental constraints.

https://doi.org/10.1017/9781009289801.010 Published online by Cambridge University Press

where $c_i = (13/15, 3, 16/3)$, $c_i' = (7/15, 3, 16/3)$, $c_i'' = (9/5, 3, 0)$ and $t = \log(Q)$. Effects of Yukawa couplings of the first two generations should be negligible, and are usually neglected in calculations, unless one is attempting to match the entire mass spectrum of SM fermions. To find the weak scale boundary conditions on the Yukawa couplings, one starts with running fermion masses (evaluated at the scale of the fermion mass) that are usually extracted in the $\overline{MS}$ (modified minimal subtraction) scheme and then converts these to corresponding masses at a scale M_Z (or m_t) in the $\overline{DR}$ scheme ($\overline{DR}$ = modified minimal subtraction using dimensional reduction). Once the running fermion masses are known at the weak scale, they can be converted to running Yukawa couplings. If $\tan\beta$ is large, it is important to include supersymmetric loop contributions to fermion masses for a reliable extraction of weak scale Yukawa couplings, especially for f_b. The Yukawa couplings can then be evolved to any other scale where the MSSM is valid using the RGEs given above. Notice that unlike the RGEs for gauge couplings that form a closed system, a knowledge of gauge couplings (but not the sparticle spectrum) is necessary to determine the Yukawa coupling evolution.

9.2.2 Evolution of soft SUSY breaking parameters

Like the gauge and Yukawa couplings, the various soft SUSY breaking parameters as well as the superpotential Higgs mass μ, evolve with energy scale. The RGE for the gaugino mass can be obtained from the generalization of the expression for the gluino mass in Eq. (8.131). Taking the derivative with respect to $t = \log(Q)$ gives,

$$\frac{\mathrm{d}M_i}{\mathrm{d}t} = \frac{g_i^2}{16\pi^2} M_i \left(-6C(G) + 2S(R)\right). \tag{9.13}$$

Exercise *Noting that the β-function for the gaugino mass is proportional to the β-function for the corresponding gauge coupling, show that*

$$\frac{M_i(Q)}{g_i^2(Q)} = K_i, \tag{9.14}$$

where the constant K_i is independent of the scale Q.

In models where the K_i defined in the last exercise are the same for each gauge group factor, we would have the relation

$$\frac{\alpha_1}{M_1} = \frac{\alpha_2}{M_2} = \frac{\alpha_3}{M_3}. \tag{9.15}$$

Such a relation is natural in many simple SUSY GUT theories. In this case, the three couplings as well as the three gaugino masses must unify at $Q = M_{\mathrm{GUT}}$, and the K_i's in Eq. (9.14) are independent of i. The relation (9.15) is therefore often

https://doi.org/10.1017/9781009289801.010 Published online by Cambridge University Press

referred to as the GUT relation for gaugino masses. We should remind the reader that the coupling α_1 is related to the conventionally normalized weak hypercharge gauge coupling α' by

$$\alpha' = \frac{3}{5}\alpha_1.$$

The one-loop RGEs for the soft SUSY breaking parameters and for μ can most easily be worked out using the analysis of Falck, and are listed below.[8] Two-loop RGEs have also been worked out; for these, we refer the reader to the original literature.[9] In writing the RGEs, we neglect any inter-generation mixing. Also, following our earlier discussion, we write the trilinear soft SUSY breaking coupling a_i as $a_i = f_i A_i$. Finally, we write the RGEs only for third generation sfermion masses and A-parameters. The corresponding RGEs for the first two generations may be obtained by self-evident replacement of the Yukawa couplings and "X" parameters (defined below). With these assumptions, the RGEs are given by,

$$\frac{\mathrm{d}M_i}{\mathrm{d}t} = \frac{2}{16\pi^2} b_i g_i^2 M_i, \tag{9.16a}$$

$$\frac{\mathrm{d}A_t}{\mathrm{d}t} = \frac{2}{16\pi^2}\left(-\sum_i c_i g_i^2 M_i + 6 f_t^2 A_t + f_b^2 A_b\right), \tag{9.16b}$$

$$\frac{\mathrm{d}A_b}{\mathrm{d}t} = \frac{2}{16\pi^2}\left(-\sum_i c_i' g_i^2 M_i + 6 f_b^2 A_b + f_t^2 A_t + f_\tau^2 A_\tau\right), \tag{9.16c}$$

$$\frac{\mathrm{d}A_\tau}{\mathrm{d}t} = \frac{2}{16\pi^2}\left(-\sum_i c_i'' g_i^2 M_i + 3 f_b^2 A_b + 4 f_\tau^2 A_\tau\right), \tag{9.16d}$$

$$\frac{\mathrm{d}B}{\mathrm{d}t} = \frac{2}{16\pi^2}\left(-\frac{3}{5}g_1^2 M_1 - 3 g_2^2 M_2 + 3 f_b^2 A_b + 3 f_t^2 A_t + f_\tau^2 A_\tau\right), \tag{9.16e}$$

$$\frac{\mathrm{d}\mu}{\mathrm{d}t} = \frac{\mu}{16\pi^2}\left(-\frac{3}{5}g_1^2 - 3 g_2^2 + 3 f_t^2 + 3 f_b^2 + f_\tau^2\right), \tag{9.16f}$$

$$\frac{\mathrm{d}m_{Q_3}^2}{\mathrm{d}t} = \frac{2}{16\pi^2}\left(-\frac{1}{15}g_1^2 M_1^2 - 3 g_2^2 M_2^2 - \frac{16}{3}g_3^2 M_3^2 + \frac{1}{10}g_1^2 S + f_t^2 X_t + f_b^2 X_b\right), \tag{9.16g}$$

$$\frac{\mathrm{d}m_{\tilde{t}_\mathrm{R}}^2}{\mathrm{d}t} = \frac{2}{16\pi^2}\left(-\frac{16}{15}g_1^2 M_1^2 - \frac{16}{3}g_3^2 M_3^2 - \frac{2}{5}g_1^2 S + 2 f_t^2 X_t\right), \tag{9.16h}$$

$$\frac{\mathrm{d}m_{\tilde{b}_\mathrm{R}}^2}{\mathrm{d}t} = \frac{2}{16\pi^2}\left(-\frac{4}{15}g_1^2 M_1^2 - \frac{16}{3}g_3^2 M_3^2 + \frac{1}{5}g_1^2 S + 2 f_b^2 X_b\right), \tag{9.16i}$$

[8] N. K. Falck, *Z. Phys.* **C30**, 247 (1986).
[9] S. Martin and M. Vaughn, *Phys. Rev.* **D50**, 2282 (1994); Y. Yamada, *Phys. Rev.* **D50**, 3537 (1994); I. Jack and D. R. T. Jones, *Phys. Lett.* **B333**, 372 (1994).

https://doi.org/10.1017/9781009289801.010 Published online by Cambridge University Press

$$\frac{\mathrm{d}m^2_{L_3}}{\mathrm{d}t} = \frac{2}{16\pi^2}\left(-\frac{3}{5}g_1^2M_1^2 - 3g_2^2M_2^2 - \frac{3}{10}g_1^2S + f_\tau^2X_\tau\right), \tag{9.16j}$$

$$\frac{\mathrm{d}m^2_{\tilde{\tau}_\mathrm{R}}}{\mathrm{d}t} = \frac{2}{16\pi^2}\left(-\frac{12}{5}g_1^2M_1^2 + \frac{3}{5}g_1^2S + 2f_\tau^2X_\tau\right), \tag{9.16k}$$

$$\frac{\mathrm{d}m^2_{H_d}}{\mathrm{d}t} = \frac{2}{16\pi^2}\left(-\frac{3}{5}g_1^2M_1^2 - 3g_2^2M_2^2 - \frac{3}{10}g_1^2S + 3f_b^2X_b + f_\tau^2X_\tau\right), \tag{9.16l}$$

$$\frac{\mathrm{d}m^2_{H_u}}{\mathrm{d}t} = \frac{2}{16\pi^2}\left(-\frac{3}{5}g_1^2M_1^2 - 3g_2^2M_2^2 + \frac{3}{10}g_1^2S + 3f_t^2X_t\right), \tag{9.16m}$$

where m_{Q_3} and m_{L_3} denote the mass term for the third generation $SU(2)$ squark and slepton doublet respectively, and

$$X_t = m^2_{Q_3} + m^2_{\tilde{t}_\mathrm{R}} + m^2_{H_u} + A_t^2, \tag{9.17a}$$

$$X_b = m^2_{Q_3} + m^2_{\tilde{b}_\mathrm{R}} + m^2_{H_d} + A_b^2, \tag{9.17b}$$

$$X_\tau = m^2_{L_3} + m^2_{\tilde{\tau}_\mathrm{R}} + m^2_{H_d} + A_\tau^2, \quad \text{and} \tag{9.17c}$$

$$S = m^2_{H_u} - m^2_{H_d} + Tr\left[\mathbf{m}_Q^2 - \mathbf{m}_L^2 - 2\mathbf{m}_U^2 + \mathbf{m}_D^2 + \mathbf{m}_E^2\right]. \tag{9.17d}$$

Here, the trace denotes a sum over generations. In many models (including the model with "universal" mass parameters to be introduced shortly), $S = 0$.

Exercise *Obtain the one-loop RGE for S and show that if S vanishes at one scale, it vanishes at all scales. We therefore do not have to worry about the S-term in the class of models where the boundary conditions ensure that S vanishes.*

Notice that the RGE for μ is completely decoupled from the soft SUSY breaking parameters, as is appropriate for a parameter occurring in the superpotential.

The complete set of 26 RGEs can be solved easily numerically as follows. Given initial values of the gauge couplings, Yukawa couplings, soft breaking terms, and μ parameter at some scale Q_0, we can plug into the right-hand side of each of the RGEs to calculate the slope, and then make a linear extrapolation along a small step size ΔQ to find new values of each of these parameters. By iterating this approach, the trajectories of each parameter can be found. In practice, more sophisticated numerical methods such as Runge–Kutta integration are used.

As an example, inspired by the apparent gauge coupling unification at the grand unified scale together with the constraints from FCNCs and electric dipole moments, we can adopt the *universality* hypothesis at the scale $Q = M_{\mathrm{GUT}} \simeq 2 \times$

https://doi.org/10.1017/9781009289801.010 Published online by Cambridge University Press

10^{16} GeV:

$$g_1 = g_2 = g_3 \equiv g_{\rm GUT}, \tag{9.18a}$$
$$M_1 = M_2 = M_3 \equiv m_{1/2}, \tag{9.18b}$$
$$m^2_{Q_i} = m^2_{U_i} = m^2_{D_i} = m^2_{L_i} = m^2_{E_i} = m^2_{H_u} = m^2_{H_d} \equiv m_0^2, \tag{9.18c}$$
$$A_t = A_b = A_\tau \equiv A_0, \tag{9.18d}$$

where all off-diagonal soft SUSY breaking scalar masses and A parameters are set to zero. Inter-generation mixing then occurs only via superpotential Yukawa couplings. Many analyses *not involving flavor physics* can be simplified by ignoring Yukawa interactions for the first two generations. Then, each generation number is separately conserved, and off-diagonal sfermion masses or A-parameters will not be generated by renormalization group evolution. Notice also that we use two notations interchangeably: m_{E_1} and $m_{\tilde{e}_{\rm R}}$ both denote the soft SUSY breaking mass for the right-handed selectron, while $m_{L_1} = m_{\tilde{e}_{\rm L}} = m_{\tilde{\nu}_{e{\rm L}}}$ denotes the common soft SUSY breaking mass parameter of the selectron, and the electron sneutrino, and similarly for squarks. The assumption that the MSSM is valid between the weak scale and GUT scale, and that the "boundary conditions" (9.18a)–(9.18d) hold is often referred to as the *mSUGRA*, or the minimal supergravity model. We will see in Chapter 11 that these boundary conditions are obtained in the simplest supergravity GUT models, assuming that below $Q = M_{\rm GUT}$, the field content is that of the MSSM.[10]

An example of the evolution of soft SUSY breaking parameters is shown in Fig. 9.7. We take $m_0 = 100$ GeV, $m_{1/2} = 200$ GeV, $A_0 = 0$, and $\tan\beta = 4$. The short dashed lines depict the running of the three gaugino masses from their common GUT scale value. The value of M_3 increases, since it has a negative β-function, while M_1 and M_2 both decrease. In the mSUGRA model, we thus expect at the weak scale the ratio of gaugino masses $M_1 : M_2 : M_3 \sim 1 : 2 :\sim 7$, in accord with the values of the weak scale gauge couplings. Thus, the gluino should be far heavier than the lighter chargino or the two lighter neutralinos.

The evolution of first generation squark and slepton mass parameters is shown by the solid lines. The evolution is solely due to their gauge interactions (Yukawa couplings are neglected) which always *increase* these masses as we run from the high scale down to the weak scale. Squark masses evolve the most because of strong interaction loop contributions to their RGEs. The small intra-generational mass splitting is due to differences in their electroweak interaction. Sleptons, because they

[10] Many phenomenological analyses of weak scale supersymmetry have been performed within this framework. Its popularity can be judged by the number of acronyms associated with it: MSSM, CMSSM, MGUM, MSGM, SSC, ... We will see in Chapter 11 that supergravity does not necessarily lead to high scale universality as was originally thought. So, rather than associating SUGRA with supergravity, one may instead consider that mSUGRA stands for *m*inimal *s*upersymmetric model with *u*niversality, *g*auge coupling unification, and *ra*diative electroweak symmetry breaking.

https://doi.org/10.1017/9781009289801.010 Published online by Cambridge University Press

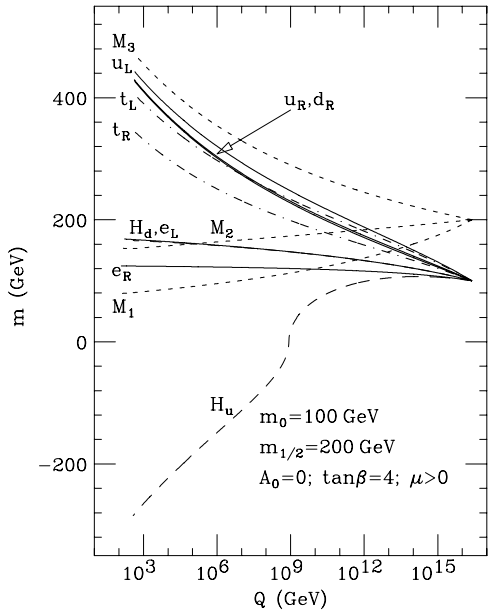

Figure 9.7 Evolution of gaugino masses, Higgs boson mass parameters, and first generation scalar mass parameters, versus energy scale in the mSUGRA model. For the scalars, we actually plot sign $(m^2) \cdot \sqrt{|m^2|}$, so that the negative values on the dashed H_u curve correspond to negative values of $m^2_{H_u}$. We use two-loop RGEs for this figure.

have just electroweak interactions, evolve much less than squarks, with $m_{\tilde{e}_R}$ evolving less than $m_{\tilde{e}_L}$ because the $SU(2)$ gauge coupling is larger than the hypercharge gauge coupling. We can see from the RGEs that the sfermion mass evolution depends on the gaugino masses which, in turn, are all proportional to $m_{1/2}$. Thus, if $m_0 \gg m_{1/2}$ most of the mass at the weak scale comes from m_0, and the sfermions will be approximately degenerate and much heavier than the gluino. If, on the other hand, $m_{1/2} \gg m_0$ as in our illustration, radiative corrections to the sfermion masses are large, and sleptons will be much lighter than the squarks, with the right selectron being the lightest of the first generation matter scalars. These important features of the soft SUSY breaking masses of the first two sfermion generations are captured by the following simple approximations to the soft terms:

$$m^2_{\tilde{q}} \simeq m_0^2 + (5-6)m^2_{1/2}, \tag{9.19a}$$

$$m^2_{\tilde{e}_L} \simeq m_0^2 + 0.5m^2_{1/2}, \tag{9.19b}$$

$$m^2_{\tilde{e}_R} \simeq m_0^2 + 0.15m^2_{1/2}, \tag{9.19c}$$

where D-term contributions given by (8.64) have been neglected for simplicity. Notice that these relations (together with the relation between M_3 and $m_{1/2}$) imply

https://doi.org/10.1017/9781009289801.010 Published online by Cambridge University Press

that the first two generations of squarks can never be much lighter than the gluino. The effect of Yukawa coupling contributions to the third generation scalar RGEs can be seen by the dot-dashed lines for the top squark soft SUSY breaking mass parameters. Yukawa interactions have an opposite effect compared to gauge interactions: they *reduce* scalar masses as we run from a high scale down to the weak scale. Indeed we see that the stop mass parameters are considerably smaller than the corresponding first generation squark masses. Remember that by $SU(2)$ invariance, $m_{\tilde{b}_L} = m_{\tilde{t}_L}$. For the low value of $\tan\beta$ used in Fig. 9.7, the bottom Yukawa coupling is small, and we expect that $m_{\tilde{b}_R} \simeq m_{\tilde{d}_R} > m_{\tilde{b}_L}$. Even though top scalars have an additional contribution m_t^2 (see (8.65a)), generally speaking these will be lighter than their first and second generation counterparts. In fact, care must be exercised to ensure that these masses do not become negative, since then charge and color breaking minima may occur in the scalar potential.

Finally, we note that because H_d and $\tilde{e}_L$ have the same gauge quantum numbers, and if bottom quark Yukawa interactions are negligible, the evolution of $m^2_{H_d}$ is virtually identical to that of $m^2_{\tilde{e}_L}$. The evolution of the Higgs mass parameter $m^2_{H_u}$ is very different and particularly noteworthy: it begins at the common GUT scale value but, because it has large top quark Yukawa interactions, it evolves to *negative* values. At first sight, something appears terribly wrong! However, as we will now see, this turns out to be just what is needed for an appropriate breakdown of electroweak symmetry.

Exercise *Notice from Fig. 9.7 that the Yukawa coupling contributions to the evolution of $m^2_{\tilde{t}_R}$, which reduce it relative to $m^2_{\tilde{u}_R}$, are larger than the corresponding contributions that reduce $m^2_{\tilde{t}_L}$. This is because the correction to $m^2_{\tilde{t}_R}$ can come from either a t_L or a b_L (or the corresponding squarks) and, respectively, the neutral or the charged component of the higgsino (scalar) component of $\hat{h}_u$, while the correction to $m_{\tilde{t}_L}$ can come only from the singlet top quark (or squark) in the loop. Since all the vertices are determined by just the superpotential top quark Yukawa coupling, we expect that the Yukawa coupling correction to $m^2_{\tilde{t}_R}$ is twice that of $m^2_{\tilde{t}_L}$. Identify this factor of two in the RGEs. Now consider the diagrams that give rise to Yukawa coupling corrections to $m^2_{H_u}$. Relative to the correction to the stop masses, how big do you expect this correction to be? Identify the corresponding term in the RGE, and check whether your answer is consistent with this.*

9.2.3 Radiative breaking of electroweak symmetry

In the SM, electroweak symmetry is spontaneously broken if a scalar field that transforms non-trivially under $SU(2)_L \times U(1)_Y$ acquires a VEV. The situation is no different in the MSSM. If the scalar field potential, evaluated at the weak scale,

https://doi.org/10.1017/9781009289801.010 Published online by Cambridge University Press

has a minimum for non-zero field values of h_u^0 or h_d^0 with zero values for other fields, we would have the desired symmetry breaking pattern. In the MSSM with arbitrary values for each of the soft SUSY breaking parameters this can be trivially arranged by choosing $m_{H_u}^2$ or $m_{H_d}^2$ to be negative. Of course, the conditions (8.17a) requiring that the origin be a maximum of the potential, and (8.17b) requiring the potential to be bounded from below need to be satisfied. The remarkable thing that we have just seen is that *even with universal mass parameters at the high scale, renormalization group evolution can cause $m_{H_u}^2$ to turn negative at the weak scale*, leaving squark and slepton squared masses to be positive. We stress that although the scalar potential with parameters renormalized at a scale $Q \gg M_{\text{weak}}$ has only positive squared masses, this does not imply that its true minimum is at the origin in field space. Radiative corrections can be substantial because of the large value of $\log(Q/M_{\text{weak}})$, and can qualitatively change this picture. Evolving the parameters of this potential to the weak scale sums these large logs, and a more reliable picture of the true potential is obtained.[11] We will, therefore, refer to this mechanism, wherein $m_{H_u}^2$ turns negative due to its renormalization group evolution, as radiative electroweak symmetry breaking (REWSB).

In Chapter 8 we minimized the tree-level scalar potential of the MSSM, and found two conditions necessary for spontaneous breaking of electroweak symmetry:

$$B = \frac{(m_{H_u}^2 + m_{H_d}^2 + 2\mu^2)\sin 2\beta}{2\mu} \quad \text{and} \tag{9.20a}$$

$$\mu^2 = \frac{m_{H_d}^2 - m_{H_u}^2 \tan^2\beta}{(\tan^2\beta - 1)} - \frac{M_Z^2}{2}. \tag{9.20b}$$

The first of these can be used to determine B (or equivalently B_0) in terms of $\tan\beta$, μ, and the Higgs mass parameters. Since B never enters the RGEs for the other parameters, its value is not needed for computing their evolution. The second of these minimization conditions determines the value of μ^2 in terms of the Higgs mass parameters and $\tan\beta$, possibly at the expense of some fine-tuning.

REWSB, which was discovered in the early 1980s,[12] occurs over a wide range of model parameters if the top quark Yukawa coupling is large enough, corresponding to $m_t \sim 100 - 200$ GeV. The subsequent discovery of the top quark with mass $m_t \simeq 175$ GeV lends credence to this mechanism. As mentioned above there are, however, regions of parameter space where charge- and color-breaking minima

[11] In practice, one usually also includes higher loop calculations and computes the minima using the effective potential as discussed in the previous chapter.

[12] L. E. Ibañez and G. G. Ross, *Phys. Lett.* **B110**, 215 (1982); K. Inoue *et al.*, *Prog. Theor. Phys.* **68**, 927 (1982) and **71**, 413 (1984); L. Ibañez, *Phys. Lett.* **B118**, 73 (1982); J. Ellis, J. Hagelin, D. Nanopoulos and M. Tamvakis, *Phys. Lett.* **B125**, 275 (1983); L. Alvarez-Gaumé, J. Polchinski and M. Wise, *Nucl. Phys.* **B221**, 495 (1983).

may occur. Thus although it is fair to say that REWSB links electroweak symmetry breaking with the breakdown of supersymmetry at some higher scale, it is premature to conclude that the *pattern* of electroweak symmetry breaking is explained.

Since REWSB is driven by the top quark Yukawa coupling, we have $m_{H_u}^2 < m_{H_d}^2$ (assuming that we start with universal masses), which implies $\tan\beta > 1$. Furthermore, in order for REWSB to be driven by the top quark Yukawa coupling, $\tan\beta$ has to be bounded above. This follows because $f_t > f_b$ implies that $m_t/m_b = f_t v_u / f_b v_d > \tan\beta$, where the Yukawa couplings, and hence the quark mass parameters, are to be evaluated at the weak scale. The bound $\tan\beta \lesssim 60$ thus obtained should be regarded as qualitative because it would be modified by radiative corrections.

The evolution of the soft SUSY breaking masses from $M_{\rm GUT}$ to the weak scale now allows us to determine the weak scale values of the soft SUSY breaking masses that are needed to determine all the sparticle masses as well as their couplings in terms of just a handful of parameters. Note that the minimization condition for REWSB specifies the value of μ^2, but not the sign of μ. It is convenient to eliminate the high scale parameter B_0 in favor of $\tan\beta$. The mSUGRA model is completely specified by the parameter set:

$$m_0,\ m_{1/2},\ A_0,\ \tan\beta, \text{sign}(\mu). \tag{9.21}$$

A selection of sparticle masses for the same mSUGRA model parameters used in Fig. 9.7 is shown in Table 9.1.

9.2.4 Naturalness constraint on superparticle masses

It is often stated loosely that sparticles ought to have masses typically below ~ 1 TeV so that the hierarchy between the SUSY breaking and weak scales can be maintained without resorting to too much fine tuning. But how much fine tuning is too much fine tuning?

To gain a better handle on how heavy sparticles can be, many groups have tried to quantify a measure of fine tuning, in order to decide which values of SUSY model parameters are natural. First, one has to decide on such a measure, and then one must decide how much fine tuning is too much. Clearly, there is a good deal of subjectivity built into constraints from naturalness. We should also keep in mind that it is possible that what appears to be fine tuning from the vantage point of the low energy theory could be the result of particular relationships in the (unknown) high energy theory. Thus, while we would regard the fine tuning required by the SM as indicative of new physics, we would not necessarily be alarmed by what appears to be fine tuning at, for instance, a part per mille level.

https://doi.org/10.1017/9781009289801.010 Published online by Cambridge University Press

Table 9.1 *Weak scale sparticle masses and parameters (GeV) for the mSUGRA model with $m_0 = 100$ GeV, $m_{1/2} = 200$ GeV, $A_0 = 0$, $\tan\beta = 4$, and $\mu > 0$. These results were obtained from the computer program ISAJET version 7.69.*

parameter	value (GeV)
$m_{\tilde{g}}$	500.5
$m_{\tilde{u}_L}$	463.4
$m_{\tilde{d}_R}$	451.7
$m_{\tilde{t}_1}$	324.7
$m_{\tilde{b}_1}$	426.9
$m_{\tilde{\ell}_L}$	176.0
$m_{\tilde{\ell}_R}$	131.0
$m_{\tilde{\tau}_1}$	129.6
$m_{\widetilde{W}_1}$	135.3
$m_{\widetilde{Z}_2}$	136.5
$m_{\widetilde{Z}_1}$	72.8
m_h	104.4
m_A	343.1
μ	292.5

A particularly simple measure of fine tuning can be extracted from the second of the electroweak symmetry breaking relations (9.20b) listed in the previous subsection. Naively, if $|\mu| \gg M_Z$, the term involving the Higgs mass parameters must also be large so that these two terms may combine and largely cancel to give M_Z. It is possible to argue that models with $|\mu| \gg M_Z$ would be fine tuned, and the weak scale value of $|\mu|$ itself can be used as a measure of fine tuning. This naive example may be too simplistic, and many authors would also argue that many parameter choices leading to $|\mu| \sim M_Z$ are also fine tuned.

As an example of a more sophisticated measure of fine tuning, we can discuss naturalness constraints in the mSUGRA model. The fundamental parameters associated with SUSY breaking are,

$$a_i = \left\{m_0,\ m_{1/2},\ A_0,\ B_0,\ \text{and}\ \mu_0\right\}. \tag{9.22}$$

Quantities associated with the weak scale can be calculated in terms of these fundamental parameters. We have included the GUT scale superpotential μ parameter in this list since we will regard the value of M_Z (which is given by the second of the electroweak symmetry breaking conditions (9.20b) mentioned above) as an output. Of course, only certain sets of GUT scale input parameters $\{a_i\}$ will give the correct value of M_Z. For variations of the input parameters $a_i \to a_i + \Delta a_i$, we can derive

https://doi.org/10.1017/9781009289801.010 Published online by Cambridge University Press

a corresponding value of $M_Z^2 + \Delta M_Z^2$. The fine-tuning requirement is that,

$$\frac{\Delta M_Z^2}{M_Z^2} < c_i \frac{\Delta a_i}{a_i},$$

where c_i is the *fine-tuning* parameter.[13] It is up to the reader to decide what constitutes an acceptable choice of c_i. Typical values quoted in the literature range from $c_i = 10$–100. Thus, if a tiny change in input parameters a_i leads to a big change in the derived value of M_Z^2 (or some other weak scale observable), then the model is said to be fine-tuned. In terms of derivatives, the fine-tuning requirement is written as

$$\left| \frac{\partial \log M_Z^2}{\partial \log a_i} \right| < c_i . \tag{9.23}$$

As an example, we show in Fig. 9.8 the m_0 vs. $m_{1/2}$ plane of the mSUGRA model, taking $A_0 = 0$, $\tan\beta = 10$, $\mu > 0$, and $m_t = 175$ GeV. The gray region in the upper left is excluded if we require that the lightest SUSY particle be electrically neutral (to fulfill cosmological constraints). The gray regions on the far right are excluded by a lack of appropriate REWSB (using the one-loop corrected scalar potential). The dark gray region for low $m_{1/2}$ is excluded in that the lightest chargino mass falls below limits from LEP2 searches: $m_{\widetilde{W}_1} < 100$ GeV. For reference, we plot also contours of $m_{\tilde{g}} = 1000$ and 2000 GeV, and $m_{\tilde{u}_L} = 1000$ and 2000 GeV. To illustrate how subjective fine-tuning considerations can be, we show examples of fine-tuning bounds obtained using various criteria for fine-tuning limits from the literature. First, we show a contour of the weak scale value of $\mu = 500$ GeV. Taking the value of μ as a fine-tuning parameter generally restricts the parameter plane to values of $m_{1/2}$ below about 400 GeV, unless m_0 is very large, in which case very large values of $m_{1/2}$ can yield "natural" models. The trajectory of constant μ is known as the hyperbolic branch (HB), and all parameter space points with low $|\mu|$ may be regarded as natural.[14] A second contour (labeled AC) was obtained by Anderson and Castaño.[15] These authors include the top Yukawa coupling f_t in the list of fundamental parameters, and use a weighted average of fine-tuning parameters to obtain their contour. Their result clearly prefers low values of both m_0 and $m_{1/2}$ to obtain natural models. Finally, a fine-tuning contour calculated by Feng, Matchev and Moroi neglects the top Yukawa coupling on the basis that it is associated with the flavor sector, and not the SUSY breaking sector.[16] Their contour (labeled FMM) excludes large $m_{1/2}$ values, but does admit solutions with

[13] R. Barbieri and G. Guidice, *Nucl. Phys.* **B306**, 63 (1988).
[14] See K. Chan, U. Chattopadhyay and P. Nath, *Phys. Rev.* **D58**, 096004 (1998).
[15] G. Anderson and D. Castaño, *Phys. Rev.* **D53**, 2403 (1996).
[16] J. L. Feng, K. T. Matchev and T. Moroi, *Phys. Rev.* **D61**, 075005 (2000).

https://doi.org/10.1017/9781009289801.010 Published online by Cambridge University Press

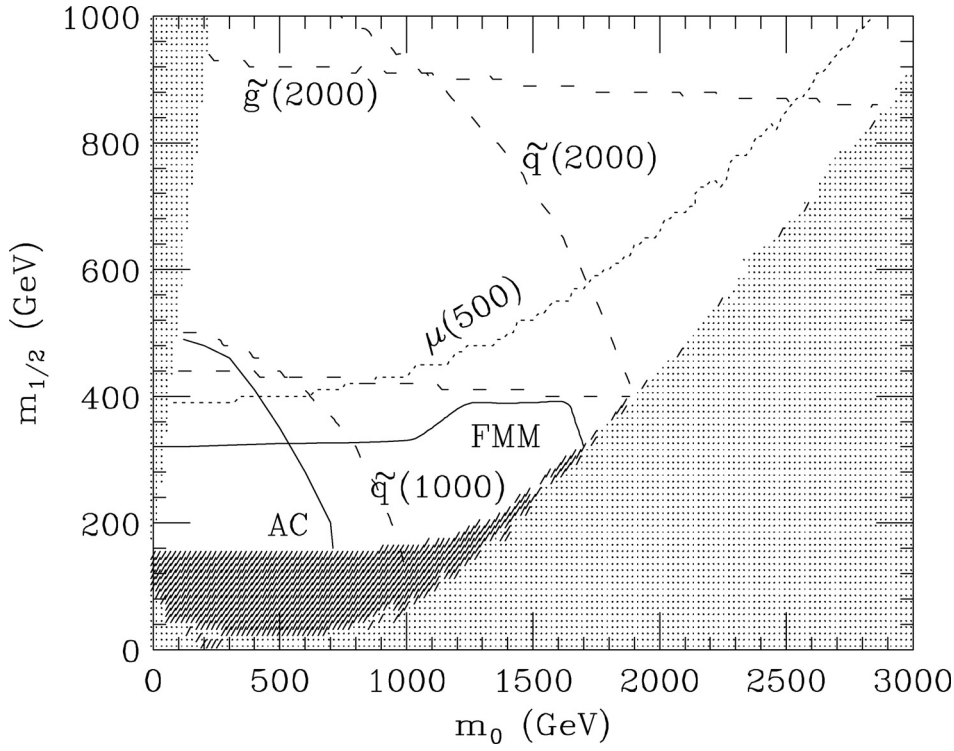

Figure 9.8 A plot of mSUGRA parameter space in the m_0 vs. $m_{1/2}$ plane, for $A_0 = 0$, $\tan\beta = 10$, and $\mu > 0$. We show contours of gluino and squark mass for 1000 and 2000 GeV. We also show sample fine-tuning contours i) $\mu = 500$ GeV, plus contours extracted from ii) Anderson and Castaño (AC), and iii) Feng, Matchev and Moroi (FMM). The proposed acceptable regions are below the fine-tuning contours.

large m_0. The large m_0 solutions have been referred to as *focus point* supersymmetry (FP), since (for $m_{1/2} \ll m_0$) the value of $m^2_{H_u}$ evolves to a fixed weak scale value independent of its GUT scale value, i.e. it is focussed in its RG trajectory. The focus point solutions offer the possibility of solving, at least partially, the SUSY flavor and *CP* problems, since in this case all the squark and slepton masses can be beyond 1 TeV while "maintaining naturalness".

9.3 Constraints from $b \to s\gamma$ decay

We have already mentioned that the agreement between the observed rate for the decay $b \to s\gamma$ and SM expectation yields significant constraints on off-diagonal squark mass squared matrix elements and **a** parameters. This should not be

https://doi.org/10.1017/9781009289801.010 Published online by Cambridge University Press

surprising because, as we saw in the exercise at the end of Section 6.6, the radiative decay of the b quark is a probe of the supersymmetry breaking sector.[17] Even in the mSUGRA model with universal GUT scalar masses and a universal A_0-parameter, significant constraints are obtained. Within this framework flavor violation, which is the other essential ingredient for this decay to occur, occurs only via Yukawa couplings. The flavor-violating matrix elements can then be calculated in terms of known quark masses and Kobayashi–Maskawa (KM) matrix elements (see exercise below). The point is that we can always go to a quark basis (at the weak scale) where the fields $u_{\rm R}$, $d_{\rm R}$, and $d_{\rm L}$ are the same as in the mass basis, while the field $u_{\rm L}$ is related to the corresponding field in the mass basis by the KM matrix. The Yukawa coupling matrices are known in this basis, and can be evolved to the high scale where the mSUGRA boundary conditions are specified. At this scale, if squarks with the same gauge quantum numbers have a common mass (the mSUGRA framework, where all squarks have a universal mass is a special case), we do not need to know the basis of squarks since all bases are equivalent. The mSUGRA boundary conditions, together with the *known* Yukawa coupling matrices thus specify the framework completely, and flavor-violating effects can be unambiguously computed.

Exercise *Unlike in the Standard Model, flavor physics is not always specified by just the Kobayashi–Maskawa matrix. A general two doublet Higgs model serves to illustrate this point. Let two $SU(2)$ doublets (H^+, H^0) and (K^+, K^0) couple the quark doublet to $d_{\rm R}$ via "Yukawa coupling matrices" $\mathbf{f_H}$ and $\mathbf{f_K}$, respectively while the conjugate doublets $(H^{0*}, -H^-)$ and $(K^{0*}, -K^-)$ respectively couple the quark doublet to $u_{\rm R}$ with Yukawa coupling matrices $\widetilde{\mathbf{f}}_{\mathbf{H}}$ and $\widetilde{\mathbf{f}}_{\mathbf{K}}$. Show that (1) the couplings of H^0 and K^0 as well as those of H^+ and K^+ to the quarks depend on all four matrices $V_{\rm L}(u)$, $V_{\rm L}(d)$, $V_{\rm R}(u)$, and $V_{\rm R}(d)$ that connect the weak current and mass bases for $u_{\rm L}$, $d_{\rm L}$, $u_{\rm R}$, and $d_{\rm R}$ type quarks (the Kobayashi–Maskawa matrix, which is determined by the couplings of quarks to $W^\pm$ bosons, is just $V_{\rm L}(u)^\dagger V_{\rm L}(d)$), and (2) the interactions of H^0 and K^0 do not conserve flavor. Verify that for the "MSSM-like case" where $\mathbf{f_K}$ and $\widetilde{\mathbf{f}}_{\mathbf{H}}$ vanish, the charged boson couplings are completely determined by the KM matrix and quark masses and, further, that the flavor-violating couplings of H^0 and K^0 vanish.*

For the case of the MSSM, some couplings involving squarks may also depend on matrices that diagonalize the squarks. It is, therefore, noteworthy that in models

[17] In practice, it is the inclusive decay $B \to X_s\gamma$ that is bounded by the experiment. The transition magnetic dipole moment operator that we argued to be absent in the SUSY limit is the operator of lowest dimensionality that could have a contribution to this decay. In principle, higher dimensional operators involving additional gluons may contribute to the inclusive decay of *B mesons* through non-renormalizable terms in the Kähler potential, but these contributions would be extremely suppressed, and quite likely smaller than the theoretical uncertainty in the calculation.

https://doi.org/10.1017/9781009289801.010 Published online by Cambridge University Press

where squarks with the same quantum numbers have a common mass at some high scale, flavor physics effects are fixed by just the KM matrix and quark masses.

In the SM the decay $b \to s\gamma$ proceeds at lowest order via a tW^- loop. In supersymmetric models, there are additional contributions from the tH^- loop, as well as sparticle loops containing $\tilde{u}_i \widetilde{W}_j$, $\tilde{d}_i \tilde{g}$, and $\tilde{d}_i \widetilde{Z}_j$. Since SM as well as SUSY contributions both occur at the one-loop level, it is reasonable to expect that if sparticles are at the weak scale, SUSY contributions to the decay amplitude will be comparable to the SM contribution, so that the experimental determination of the branching ratio will provide strong constraints on the parameters of supersymmetric models.

The $b \to s\gamma$ decay rate is usually calculated by evaluating lowest order matrix elements of effective theory operators at a scale $Q \sim m_b$. The complete calculation is complicated by the fact that QCD corrections are large. These are included via renormalization group resummation of leading logs (LL) which arise due to a disparity between the scale at which new physics enters the $b \to s\gamma$ loop corrections (usually taken to be $Q \sim M_W$), and the scale at which the $b \to s\gamma$ decay rate is evaluated ($Q \sim m_b$). The resummation is most easily performed within the framework of effective field theories. Above the scale $Q = M_W$ (all scales $Q \sim M_W$ are equivalent in LL perturbation theory), calculations are performed within the full theory. Below $Q = M_W$, particles heavier than M_W are integrated out, leading to an effective Hamiltonian,

$$H_{\text{eff}} = -\frac{4G_F}{\sqrt{2}} V_{tb} V_{ts}^* \sum_{i=1}^{8} C_i(Q) O_i(Q). \tag{9.24}$$

Matching the two theories at $Q = M_W$ yields the values of the so-called Wilson coefficients $C_i(Q = M_W)$. The O_i in Eq. (9.24) are a complete set of operators that mix via QCD; their form can be found in the literature.[18] The logs are summed by solving the renormalization group equations (RGEs) for the Wilson coefficients

$$Q \frac{\mathrm{d}}{\mathrm{d}Q} C_i(Q) = \gamma_{ji} C_j(Q), \tag{9.25}$$

where γ is the 8×8 anomalous dimension matrix. The matrix elements of the operators O_i are finally calculated at a scale $Q \sim m_b$ and multiplied by the appropriately evolved Wilson coefficients to obtain the decay amplitude. The LL QCD corrections just described yield enhancements in the $b \to s\gamma$ decay rate of factors of 2–5. Variation of the scale choice between $m_b/2 < Q < 2m_b$ yields approximately a 25% uncertainty in the theoretical calculation. This is reduced to about 9% by working at next-to-leading order. We also note that the SUSY

[18] See e.g., G. Buchalla, A. Buras and M. Lautenbacher, *Rev. Mod. Phys.* **68**, 1125 (1996).

https://doi.org/10.1017/9781009289801.010 Published online by Cambridge University Press

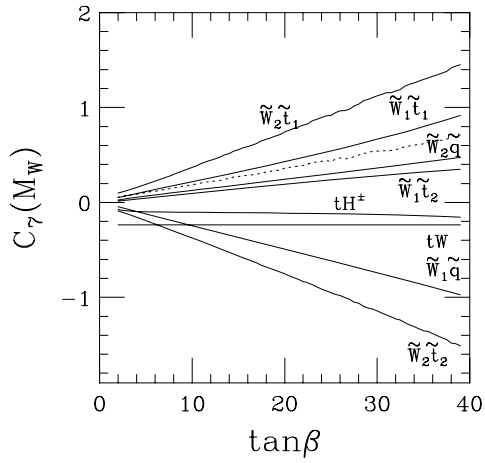

Figure 9.9 Contributions to the Wilson coefficient $C_7(M_W)$ versus $\tan\beta$ from various loop contributions. We take $m_0 = 100$ GeV, $m_{1/2} = 200$ GeV, $A_0 = 0$, and $\mu > 0$. The dotted line shows the total contribution from sparticle loops. Reprinted with permission from H. Baer, M. Brhlik, D. Castaño and X. Tata, *Phys. Rev.* **D58**, 015007 (1998), copyright (1998) by the American Physical Society.

calculation has larger uncertainty, especially if $\tan\beta$ is large. Our discussion here is to give the reader a flavor of the ingredients that go into such a calculation. These calculations are sophisticated, and the reader who is actually interested in performing the calculation is well advised to consult the original literature.

The most important of the above operators is the magnetic operator $O_7 \sim \overline{s}_L \sigma^{\mu\nu} b_R F_{\mu\nu}$. In Fig. 9.9, we show the magnitude of the Wilson coefficient $C_7(M_W)$ versus $\tan\beta$ from various contributions involving tW, tH^-, and $\widetilde{W}_i\tilde{q}_j$ loops for one choice of mSUGRA parameters. The total contribution from gluino and neutralino loops is negligible. We see from the figure that large cancellations are possible between the various contributions.

In Fig. 9.10, we show the $b \to s\gamma$ branching fraction contours in the m_0 vs. $m_{1/2}$ plane, for $\tan\beta = 10$, $A_0 = 0$, and *a*) $\mu < 0$ and *b*) $\mu > 0$. Data from the CLEO, BELLE, and ALEPH experiments, roughly speaking, restrict $2 \times 10^{-4} \lesssim B(b \to s\gamma) \lesssim 5 \times 10^{-4}$, if we conservatively factor in theoretical uncertainties. Clearly, the mSUGRA model with $\mu < 0$ is only consistent with data for large values of $m_{1/2} > 300$ GeV. For $\mu > 0$, virtually the entire plane is allowed. Qualitatively similar results are obtained for even larger values of $\tan\beta$.

9.4 $B_s \to \mu^+\mu^-$ decay

Within the framework of the Minimal Supersymmetric Standard Model (MSSM), FCNC conservation is ensured (at tree level) by requiring that the matter multiplets

https://doi.org/10.1017/9781009289801.010 Published online by Cambridge University Press

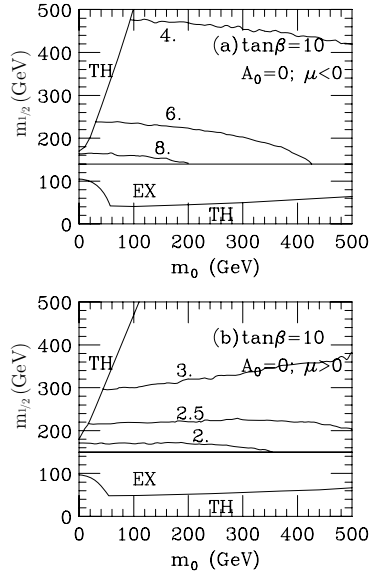

Figure 9.10 Contours of constant branching fraction $B(b \to s\gamma)$ in the m_0 vs. $m_{1/2}$ plane for $\tan\beta = 10$, $A_0 = 0$. The number labeling each contour must be multiplied by 10^{-4} to obtain the branching fraction. The region labeled EX is excluded by the constraint $m_{\widetilde{W}_1} > 100$ GeV while the region marked TH is not allowed for theoretical reasons.

with weak isospin $T_3 = 1/2$ couple only to the Higgs superfield $\hat{H}_u$, while those with $T_3 = -1/2$ couple just to the Higgs superfield $\hat{H}_d$.

At the one-loop level, however, a coupling of $\hat{H}_u$ to down-type fermions is induced. This induced coupling leads to a new contribution, proportional to v_u, to the down-type fermion mass matrix. Although this contribution is suppressed by a loop factor relative to the tree-level contribution, this suppression is (partially) compensated if $\tan\beta$ is sufficiently large. As a result, down-type Yukawa interactions and down-type quark mass matrices are no longer diagonalized by the same transformation, and flavor-violating couplings of neutral Higgs scalars h, H, and A emerge. In the limit of large m_A, the Higgs sector becomes equivalent to the Standard Model (SM) Higgs sector with a light Higgs boson $h \simeq H_{\rm SM}$, and the effects of flavor violation decouple from the low energy theory . The interesting feature is that the flavor-violating couplings of h, H, and A *do not decouple for large superparticle mass parameters*: being dimensionless, these couplings depend only on ratios of these mass parameters, and so remain finite even for very large values of SUSY mass parameters.[19] This flavor-violating neutral Higgs boson coupling results in a potentially observable branching fraction for the decay $B_s \to \mu^+\mu^-$

[19] These not only include sparticle masses, but also the superpotential parameter μ and also the soft SUSY breaking A-parameters.

https://doi.org/10.1017/9781009289801.010 Published online by Cambridge University Press

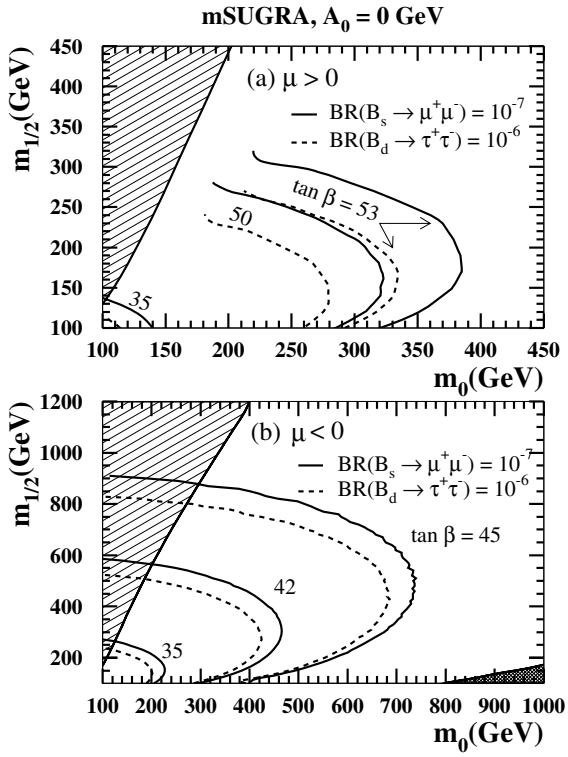

Figure 9.11 Contours of $B(B_s \to \mu^+\mu^-) = 10^{-7}$ (solid) and $B(B_d \to \tau^+\tau^-) = 10^{-6}$ (dashed) in the m_0 vs. $m_{1/2}$ plane of the mSUGRA model for several values of $\tan\beta$ and (*a*) $\mu > 0$, and (*b*) $\mu < 0$. In frame (*a*), the contours end where $\widetilde{Z}_1$ is no longer the LSP. The region where this occurs for $\tan\beta = 35$ is shaded. Reprinted with permission from J. K. Mizukoshi, X. Tata, and Y. Wang, *Phys. Rev* **D66**, 115003 (2002), copyright (2002) by the American Physical Society.

mediated by the neutral Higgs bosons, h, H, and A, and possibly also the decay $B_d \to \tau^+\tau^-$.[20] The former might be probed at the Tevatron (the CDF experiment has already limited it to be $< 5.8 \times 10^{-7}$), while the latter might be detectable at B-factories. Within the MSSM, this branching fraction – which depends sensitively on $\tan\beta$ and m_A and less sensitively on other sparticle masses – can be more than 1000 times its SM value.

In Fig. 9.11 we illustrate the branching fraction for these Higgs-mediated leptonic decays of B_s and B_d mesons within the mSUGRA framework for *a*) $\mu > 0$, and *b*) $\mu < 0$. The solid lines show contours of $B(B_s \to \mu^+\mu^-) = 10^{-7}$, a level that Tevatron experiments should probe with an integrated luminosity ~ 2 fb^{-1}, for the values of $\tan\beta$ shown on the contours. The dashed lines are contours of $B(B_d \to \tau^+\tau^-) = 10^{-6}$. The contours in frame *a*) end where $\widetilde{Z}_1$ is no longer the LSP. If

[20] See, e.g., K. S. Babu and C. Kolda, *Phys. Rev. Lett.* **84**, 228 (2000).

https://doi.org/10.1017/9781009289801.010 Published online by Cambridge University Press

$\tan\beta$ is sufficiently large, Tevatron experiments will probe SUSY via B_s decays for parameter ranges where signals from direct production studied in Chapter 15 are predicted to be below the detectable level. The sensitivity of B-factories to $B(B_d \to \tau^+\tau^-)$ is not known.

9.5 Muon anomalous magnetic moment

Historically, the anomalous magnetic moment of the electron has been a harbinger of new physics, from the advent of the Dirac theory of the electron to the formulation of QED, and up to the present day. For contemporary new physics searches, the anomalous magnetic moment of the muon (rather than the better measured moment of the electron) turns out to have greater importance because for many extensions of the SM the new physics contributions to the lepton magnetic moment are proportional to m_ℓ^2. The E821 experiment at Brookhaven National Laboratory has measured $a_\mu = (g-2)_\mu/2$ to eight significant figures, with a precision better than a part per million.[21] In the SM, QED corrections to the photon–muon–muon vertex have been calculated to four loops (with an estimate for the fifth-loop contribution, showing that its magnitude is small for the purpose of our analysis). Electroweak corrections, which are significant, have also been calculated. The biggest theoretical uncertainty comes from hadronic corrections. Although there is some controversy about the magnitude of the theoretical uncertainty, it is comparable to or better than the experimental uncertainty. If weak scale SUSY exists, then there will also be SUSY contributions to a_μ via the $\widetilde{W}_i - \tilde{\nu}_\mu$ and $\widetilde{Z}_i - \tilde{\mu}_j$ loops shown in Fig. 9.12. The SUSY contribution gives

$$\Delta a_\mu^{\rm SUSY} \propto \frac{m_\mu^2 \mu M_i \tan\beta}{M_{\rm SUSY}^4}, \tag{9.26}$$

where M_i $(i = 1, 2)$ is a gaugino mass and $M_{\rm SUSY}$ is a characteristic sparticle mass circulating in the loop. The complete one-loop result is given, for instance, by Moroi.[22] We see that $\Delta a_\mu^{\rm SUSY}$ grows with $\tan\beta$ and, for models with a positive gaugino mass, has the same sign as the superpotential Higgs mass term μ. Depending on SUSY parameters, its magnitude may be comparable to that of the weak contribution, so that the sensitivity of the E821 experiment is at a level where it can probe these SUSY contributions.

[21] See e.g. G. W. Bennett *et al.* (Muon $g-2$ Collaboration), hep-ex/0401008.

[22] T. Moroi, *Phys. Rev.* **D53**, 6565 (1996). That the SUSY contributions to a_μ cancel the corresponding SM contributions in the SUSY limit of the MSSM – this limit is discussed in the exercise at the end of Section 8.3.6 – in accord with the general result demonstrated in the exercise at the end of Section 6.6 has been explicitly demonstrated at the one-loop level by T. Ibrahim and P. Nath, *Phys. Rev.* **D61**, 095008 (2000).

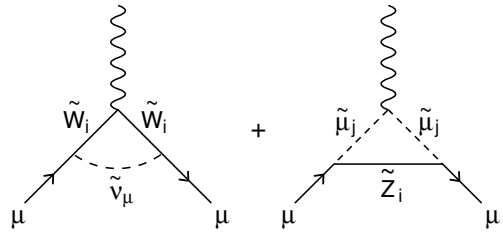

Figure 9.12 Supersymmetric contributions to $g-2$ of the muon.

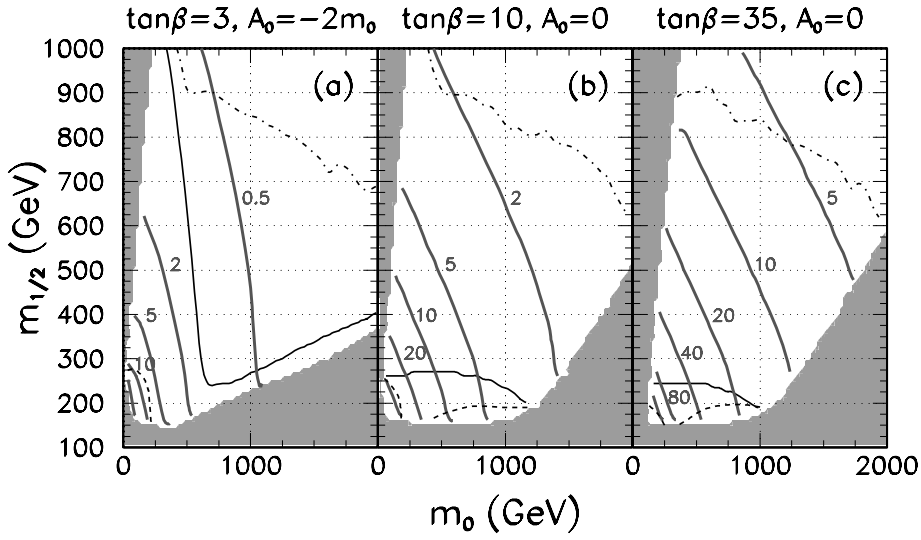

Figure 9.13 Contours of $a_\mu \times 10^{10}$ in the mSUGRA model for $\mu > 0$. The Fermilab Tevatron (dashes) and CERN LHC (dot-dashed) reach contours are also shown.

Contours of $\Delta a_\mu^{\rm SUSY} \times 10^{10}$ are shown in Fig. 9.13 for three $\tan\beta$ values in the mSUGRA model, and $\mu > 0$. Regions of parameter space where $\Delta a_\mu^{\rm SUSY} \gtrsim 60 \times 10^{-10}$ and $\Delta a_\mu^{\rm SUSY} < 0$ are currently disfavored. As the experimental error reduces, and theoretical calculations improve, the results will more definitively point to preferred and excluded regions of SUSY model parameter space.

9.6 Cosmological implications

Since R-parity is assumed to be conserved in the MSSM, the lightest SUSY particle is absolutely stable. This has profound implications for cosmology and, in particular, may imply that relic LSPs left over from the Big Bang could account for the bulk of the matter in the Universe. Moreover, the requirement that the relic density

https://doi.org/10.1017/9781009289801.010 Published online by Cambridge University Press

of LSPs should be in accord with astrophysical measurements of the dark matter density of the Universe leads to important constraints on supersymmetric model parameters.

The central idea behind relic density calculations is that in the very early Universe, when temperatures were very hot (i.e. $T \gg m_{\rm LSP}$, where the Boltzmann constant $k = 1$), neutralinos were being created and annihilated, but that they were in a state of thermal equilibrium with the cosmic soup. As the Universe expanded, and cooled, its temperature dropped below the level where LSPs could be pair-produced, although they could still annihilate one with another. Ultimately, the expansion rate of the Universe outstripped the LSP annihilation rate, and (except for dilution due to the expansion of the Universe) the relic density of LSPs was locked in. Thus, if the MSSM and the basic Big Bang picture are both correct, a gas of LSPs should fill all space, and could account for much of the missing matter of the Universe. Such a scenario immediately rules out almost all cases of having a colored or electrically charged LSP, since otherwise such relics would have become bound to nuclei and atoms, and would have been detected in search experiments for anomalous nuclei and atoms: searches for anomalous isotopes are sensitive to an isotope abundance ranging between 10^{-12}–10^{-29} depending on the isotope,[23] to be compared with a theoretical expectation of 10^{-6}–10^{-10} for an LSP mass of 100–1000 GeV.[24] Within the MSSM framework, this leaves a sneutrino or the lightest neutralino as candidates for the LSP.

Many experiments have searched for such weakly interacting massive particles (WIMPs) as relic dark matter from the Big Bang. The basic idea is to detect collisions of WIMPs with nuclei of detector material. If the WIMP is the lightest neutralino with a mass $\sim$ 100 GeV, then a typical neutralino-nucleus elastic scattering will involve energies of a few keV. To detect such tiny energy depositions, detector materials are frequently cooled to ultra-low temperatures, so that phonons, ionization or superconducting phase transitions can be detected. If instead the WIMP is a sneutrino heavier than about 25 GeV, then it should have been seen already by such direct dark matter detection experiments. Sneutrinos lighter than $\sim$ 25 GeV are excluded by measurements of the properties of the Z boson at LEP (and also by the non-observation of energetic solar neutrinos in the Kamiokande detector). Thus, cosmological considerations point to the lightest neutralino, $\widetilde{Z}_1$, as being the LSP for the MSSM. It is satisfying that in most model calculations (see Chapter 11) involving the MSSM, the lightest neutralino is in fact the LSP.

[23] See e.g. T. Hemmick *et al.*, *Phys. Rev.* **D41**, 2074 (1990) and references therein.
[24] S. Wolfram, *Phys. Lett.* **B82**, 65 (1979); C. B. Dover, T. Gaisser and G. Steigman, *Phys. Rev. Lett.* **42**, 1117 (1979).

Another possibility is that the LSP is the gravitino.[25] In this case, gravitinos could account for the cold dark matter (CDM) in the Universe, but direct or indirect gravitino detection would likely be impossible.

9.6.1 Relic density of neutralinos

The total matter/energy density $\Omega = \rho/\rho_c$ of the Universe is usually written as a fraction in terms of the critical closure density $\rho_c = 3H_0^2/8\pi G_N \simeq 1.88 \times 10^{-29} h^2$ g cm^{-3}. Here, $H_0 \simeq 71$ km s^{-1} Mpc^{-1} is the value of the Hubble parameter today, and G_N is Newton's gravitational constant. H_0 is frequently parametrized as $H_0 \equiv 100h$ km s^{-1} Mpc^{-1}, where h is a dimensionless scaling constant.

The past decade has witnessed increasingly precise measurements of the anisotropies of the cosmic microwave background (CMB) radiation left over from the Big Bang. Recent results come from the Wilkinson Microwave Anisotropy Probe (WMAP) satellite measurements. Astonishingly, an analysis of their results pinpoints the age of the Universe to be 13.7 ± 0.2 Gyrs.[26] In addition, the geometry of the Universe is flat, consistent with simple inflationary models. The dark energy content of the Universe is found to be about 73%, while the matter content is about 27%. A best fit of WMAP and other data sets to cosmological parameters in the ΛCDM cosmological model yields a determination of baryonic matter density $\Omega_b h^2 = 0.0224 \pm 0.0009$, which is in excellent agreement with estimates from Big Bang nucleosynthesis, a total matter density of $\Omega_m h^2 = 0.135^{+0.008}_{-0.009}$, and a very low density of hot dark matter (relic neutrinos). From these values the cold dark matter density of $\Omega_{\rm CDM} h^2 = 0.1126^{+0.0161}_{-0.0181}$ (at 2σ) can be inferred.

The discrepancy between baryonic and total matter density may come from CDM particles (that is, non-relativistic matter that does not radiate light), while the remaining energy density may come from a non-zero cosmological constant, as was first suggested by measurements of type Ia supernovae at the highest red shifts, and then strikingly confirmed by the CMB data. We will see that the lightest neutralino of supersymmetry can be an excellent candidate for CDM in the Universe.

The relic density of neutralinos predicted by the MSSM can be found by solving the Boltzmann equation as formulated for a Friedmann–Robertson–Walker (FRW) Universe:

$$\frac{dn}{dt} = -3Hn - \langle \sigma v_{\rm rel} \rangle (n^2 - n_0^2). \tag{9.27}$$

Here, n is the number density of neutralinos, t is time, n_0 is the thermal equilibrium number density, and $\langle \sigma v_{\rm rel} \rangle$ is the thermally averaged neutralino annihilation cross

[25] For a discussion of this possibility, see J. Feng, S. Su and F. Takayama, hep-ph/0404231, and references therein.
[26] See e.g. D. N. Spergel *et al.* (WMAP Collaboration), *Astrophys. J. Suppl.* **148**, 175 (2003).

https://doi.org/10.1017/9781009289801.010 Published online by Cambridge University Press

section times relative velocity. (Remember that except for s-wave scattering, $\sigma v_{\rm rel}$ depends on $v_{\rm rel}$, so that the thermal average depends on the temperature.) The first term on the right represents a diminution of number density as the Universe expands, while the second term represents the change due to annihilation of neutralinos into SM particles.

Using conservation of entropy and the kinematics of a FRW Universe, it is convenient to reparametrize the Boltzmann equation in terms of temperature rather than time. In the radiation dominated era, the entropy density $\propto T^3$, so that the size of the Universe $R \propto 1/T$, and $t \simeq 1/(2H) = \sqrt{\frac{45}{16\pi^3 g_* G_{\rm N}}}\frac{1}{T^2}$, where $g_* \sim 80$ counts the total number of relativistic degrees of freedom.[27] Defining $f = n/T^3$ and rescaling the temperature in terms of particle mass, $x = T/m$, the Boltzmann equation can be recast in the form

$$\frac{{\rm d}f}{{\rm d}x} = m\sqrt{\frac{45}{4\pi^3 g_* G_{\rm N}}}\langle\sigma v_{\rm rel}\rangle(f^2 - f_0^2). \tag{9.28}$$

The Boltzmann equation can be solved in several steps.

1. At very early times the last term in (9.27) dominates, and n is close to its equilibrium value, so that $f \simeq f_0$. For non-relativistic particles (including their rest mass), $E \simeq m + p^2/2m$, and the equilibrium number density is given by

$$\begin{aligned} f_0(x) = \frac{n_0}{T^3} &= \frac{1}{T^3}\frac{g}{(2\pi)^3}\int {\rm d}^3 p {\rm e}^{-E/T} \\ &= \frac{1}{T^3}\frac{4\pi g}{(2\pi)^3}{\rm e}^{-m/T}\int_0^\infty p^2 {\rm d}p {\rm e}^{-p^2/2mT} \\ &= \frac{g}{2}\sqrt{\frac{1}{2\pi^3}}(\frac{m}{T})^{\frac{3}{2}}{\rm e}^{-\frac{m}{T}} \\ &= \frac{g}{2}\sqrt{\frac{1}{2\pi^3}}x^{-\frac{3}{2}}{\rm e}^{-\frac{1}{x}}, \end{aligned} \tag{9.29}$$

   where $g = 2$ is the number of spin degrees of freedom for a neutralino.
2. As the Universe cools to temperatures below $T = m$, the number density of neutralinos falls exponentially. However, if this would continue, neutralinos would no longer be able to annihilate efficiently, and the first term on the right-hand side of the Boltzmann equation would begin to dominate. In this regime, we would have

$$\frac{1}{n}\frac{{\rm d}n}{{\rm d}t} = -3\frac{1}{R}\frac{{\rm d}R}{{\rm d}t},$$

[27] E. W. Kolb and M. S. Turner, *The Early Universe*, Addison-Wesley (1990).

https://doi.org/10.1017/9781009289801.010 Published online by Cambridge University Press

so that $n \propto 1/R^3$: i.e. the number density of neutralinos would reduce only due to the expansion of the Universe, and no longer drop exponentially. In other words, the number of neutralinos would be much larger than expected from thermal equilibrium. This is referred to as freeze out. The temperature at which this occurs may be estimated by using the equilibrium f on the left-hand side of (9.28) and setting $f^2 - f_0^2 \simeq f_0^2$ on its right-hand side. This then gives the freeze out temperature,

$$1/x_F = \log\left[\frac{m}{2\pi^3}\sqrt{\frac{45}{2g_* G_{\rm N}}}\langle\sigma v_{\rm rel}\rangle\sqrt{x_{\rm F}}\right]. \tag{9.30}$$

This equation can be solved iteratively, and typically yields $T_{\rm F} \simeq m/20$.

3. With the relic density locked in at a value much larger than its value in thermal equilibrium, $f^2 \gg f_0^2$, we can integrate the Boltzmann equation to obtain the relic density *today* as,

$$n(T_0) = \frac{1}{m}\left(\frac{T_0}{T_\gamma}\right)^3 (T_\gamma)^3\sqrt{\frac{4\pi^3 g_* G_{\rm N}}{45}}\left[\int_0^{x_{\rm F}}\langle\sigma v_{\rm rel}\rangle {\rm d}x\right]^{-1}, \tag{9.31}$$

where $T_\gamma = 2.75$ K is today's cosmic microwave background temperature. We see that the relic number density $\propto T^3$ showing that it is indeed dropping only due to the expansion of the Universe as discussed above. The reason for writing the relic density in this form is that we do not know the neutralino temperature T_0: but for the fact that photons are reheated as species decouple, these two temperatures would be the same. Since the reheating process is isentropic, and $s = gT^3$, $(T_\gamma/T_0)^3$ can be obtained from the ratio of the number of degrees of freedom at freeze out to the effective number of degrees of freedom today and is approximately equal to 19.4.

The neutralino relic density can be recast in the form

$$\Omega_{\tilde{Z}_1} h^2 = \frac{\rho_{\tilde{Z}_1}(T_0)}{8.1\times 10^{-47}\ {\rm GeV}^4}, \tag{9.32}$$

with $\rho_{\tilde{Z}_1} = mn(T_0)$ given by,

$$\rho_{\tilde{Z}_1}(T_0) \simeq \frac{1.66}{M_{\rm Pl}}\left(\frac{T_0}{T_\gamma}\right)^3 T_\gamma^3\sqrt{g_*}\frac{1}{\int_0^{X_{\rm F}}\langle\sigma v_{\rm rel}\rangle {\rm d}x}. \tag{9.33}$$

Central to the calculation is the evaluation of the thermally averaged neutralino annihilation cross section times velocity. This has been simplified to a one-dimensional

https://doi.org/10.1017/9781009289801.010 Published online by Cambridge University Press

integral by Gondolo and Gelmini:[28]

$$\langle \sigma v_{\rm rel} \rangle = \frac{\int \sigma v_{\rm rel} e^{-E_1/T} e^{-E_2/T} d^3p_1 d^3p_2}{\int e^{-E_1/T} e^{-E_2/T} d^3p_1 d^3p_2}$$
$$= \frac{1}{4x K_2^2(\frac{1}{x})} \int_2^\infty da \sigma(a) a^2 (a^2-4) K_1(\frac{a}{4}), \qquad (9.34)$$

where $a = \sqrt{s}/m_{\widetilde{Z}_1}$ and K_i are modified Bessel functions of order i. Evaluation of the relic density thus requires the knowledge of all neutralino annihilation cross sections $\widetilde{Z}_1\widetilde{Z}_1 \to f_1 f_2$, where f_1 and f_2 are SM particles. How to compute cross sections, starting with the interactions derived in the last chapter, will be discussed in Chapter 12.

If there are other sparticles with mass close to the LSP mass, these will also be present in the thermal bath right up to the time that the LSP decouples. In this case, it is necessary to take into account SUSY processes involving annihilation of pairs of these sparticles as well as co-annihilation of these sparticles and the LSP to accurately obtain the neutralino relic density. Although the number density of the heavier sparticles is suppressed by the Boltzmann factor $\exp(-m/T)$, this may be compensated for by the fact that the cross sections for co-annihilation or pair annihilation may be much larger than the LSP annihilation cross section. For instance, if the $\tilde{\tau}_1$ is close in mass to a gaugino-like $\widetilde{Z}_1$, its annihilation rate may be much larger than the annihilation rate for $\widetilde{Z}_1$ pairs. Alternatively, in models with small values of μ, $m_{\widetilde{Z}_1} \sim m_{\widetilde{Z}_2} \sim m_{\widetilde{W}_1}$, and $\sigma_{\widetilde{Z}_1\widetilde{Z}_2}$ or $\sigma_{\widetilde{W}_1\widetilde{W}_1}$ (which are not P-wave suppressed at threshold) may be much larger than the annihilation cross section for two $\widetilde{Z}_1$s.

The WMAP determination $\Omega_{\rm CDM}h^2 = 0.1126^{+0.0161}_{-0.0181}$ implies an upper limit $\Omega_{\rm WIMP}h^2 < 0.129$ (2σ) on the relic density of any stable WIMP. Only if we further assume that the cold dark matter consists solely of a single component can we infer that the relic density of any particular WIMP (in our case $\Omega_{\widetilde{Z}_1}h^2$) will saturate the WMAP value. In Fig. 9.14, we show regions of relic density $\Omega_{\widetilde{Z}_1}h^2$ in the m_0 vs. $m_{1/2}$ plane for (*a*) $\tan\beta = 10$ and $\mu > 0$ and (*b*) $\tan\beta = 45$ for $\mu < 0$, where $A_0 = 0$ and $m_t = 175$ GeV. The very dark gray regions on the right and far left are excluded by either not having a neutralino LSP, or not having the correct EWSB pattern. The white regions for both $\tan\beta$ values have $\Omega_{\widetilde{Z}_1}h^2 > 1$, so that the Universe would be younger than 10 billion years. The appropriately labeled light gray region is where $\Omega_{\widetilde{Z}_1}h^2 \leq 0.1$, and can be regarded as the theoretically favored region. Four regions of parameter space emerge with $\Omega_{\widetilde{Z}_1}h^2 < 0.129$, as determined by the WMAP analysis. In frame (*a*), we see:

[28] P. Gondolo and G. Gelmini, *Nucl. Phys.* **B360**, 145 (1991). Formulae including co-annihilation effects can be found in J. Edsjo and P. Gondolo, *Phys. Rev.* **D56**, 1879 (1997).

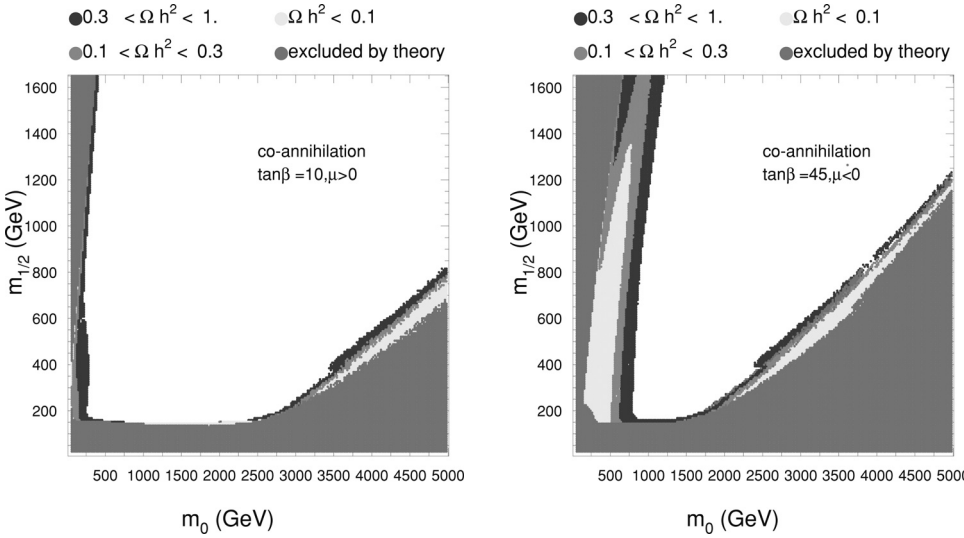

Figure 9.14 Predictions for neutralino relic density $\Omega_{\widetilde{Z}_1}h^2$ in the m_0–$m_{1/2}$ plane of the mSUGRA model for $\mu > 0$ and two values of $\tan\beta$. We thank A. Belyaev for supplying this figure.

- the bulk annihilation region,
- the stau co-annihilation region, and
- the HB/FP region.

In addition, in frame (*b*), we see

- the A-annihilation funnel.

The bulk annihilation region occurs at low m_0 and low $m_{1/2}$ where neutralino annihilation mainly occurs via $\widetilde{Z}_1\widetilde{Z}_1 \to \ell\bar{\ell}$, via t-channel slepton exchange. As m_0 increases, the slepton masses also increase, suppressing the neutralino annihilation rate and increasing the relic density. The stau co-annihilation region is the narrow corridor of favored relic density adjacent to the region where $\tilde{\tau}_1$ becomes the LSP; this is where $\widetilde{Z}_1\tilde{\tau}_1$ and $\tilde{\tau}_1\bar{\tilde{\tau}}_1$ co-annihilation can take place. The HB/FP region occurs at large m_0 along the lack of REWSB excluded region. In this area, since $|\mu|$ is becoming small, the $\widetilde{Z}_1$ becomes increasingly higgsino-like, and annihilation into WW, ZZ, and Zh states becomes large. Directly adjacent to the REWSB excluded region, where $\mu \to 0$, co-annihilation of $\widetilde{Z}_1$ with $\widetilde{W}_1$ and $\widetilde{Z}_2$ is also important. There is also a narrow strip of low relic density at $m_{1/2} \sim 160$ GeV just beyond the reach of LEP2 where neutralino annihilation via the narrow light Higgs h resonance occurs: $\widetilde{Z}_1\widetilde{Z}_1 \to h \to b\bar{b},\ \tau\bar{\tau}$.

https://doi.org/10.1017/9781009289801.010 Published online by Cambridge University Press

Frame (b) is qualitatively different from frame (a) in that there is a broad corridor of very low relic density adjacent to the stau co-annihilation region. This occurs when $\widetilde{Z}_1\widetilde{Z}_1 \to A \to b\bar{b},\ \tau\bar{\tau}$ annihilation is enhanced at large tan β. The annihilation rate is enhanced in part because at large tan β, the value of m_A can decrease to the extent that resonance annihilation can take place. It is also enhanced because the b- and τ-Yukawa couplings become large. Resonance annihilation also takes place via the heavy Higgs H, but this is somewhat suppressed relative to annihilation through A. Moreover, at these very large values of tan β, the Higgs bosons H and A become very broad ($\Gamma_{H,A} \sim$ 10–50 GeV), so that the resonance annihilation corridor becomes very broad, and in fact contributes to the annihilation cross section across the entire plane.

9.6.2 Direct detection of neutralino dark matter

If SUSY dark matter exists, then a non-relativistic gas of LSPs fills all space. Moreover, the LSPs are gravitationally clumped to form a galactic dark matter halo. A number of direct WIMP detection experiments have been built or are under construction to detect this halo. The general idea behind these experiments is that as the earth moves through this halo, relic WIMPs, be they neutralinos or something else, will scatter off the nuclei in some material, depositing typically tens of keV of energy. The energy that is deposited could be detected via: (i) changes in resistance due to a slight temperature increase (bolometry), (ii) a magnetic flux change due to a superconducting granule phase transition, (iii) ionization, or (iv) phonons.[29] Sneutrinos have a large scattering cross section, and it is the lack of a signal in such experiments that disfavors the sneutrino as the LSP. Neutralino cross sections are much smaller, and require higher sensitivity for their detection. Gravitinos are essentially undetectable. The technical challenge is to build detectors that could pick out the relatively rare, low energy neutralino scattering events from backgrounds mainly due to cosmic rays and radioactivity in surrounding matter. Future detectors are aiming to reach a sensitivity of 0.01–0.001 events kg^{-1} day^{-1}. It is possible that the first evidence for SUSY may come from direct neutralino detection rather than from accelerator experiments, though identifying the SUSY origin of the signal may require other analyses.

The first step involved in a neutralino–nucleus scattering calculation is to calculate the effective four-particle neutralino–quark and neutralino–gluon interactions. The neutralino–quark axial vector interaction leads, in the non-relativistic limit, to a neutralino–nucleon spin-spin interaction, which involves the measured quark spin content of the nucleon. To obtain the neutralino–nucleus scattering cross section, a

[29] For a review, see G. Jungman, M. Kamionkowski and K. Griest, *Phys. Rep.* **267**, 195 (1996).

https://doi.org/10.1017/9781009289801.010 Published online by Cambridge University Press

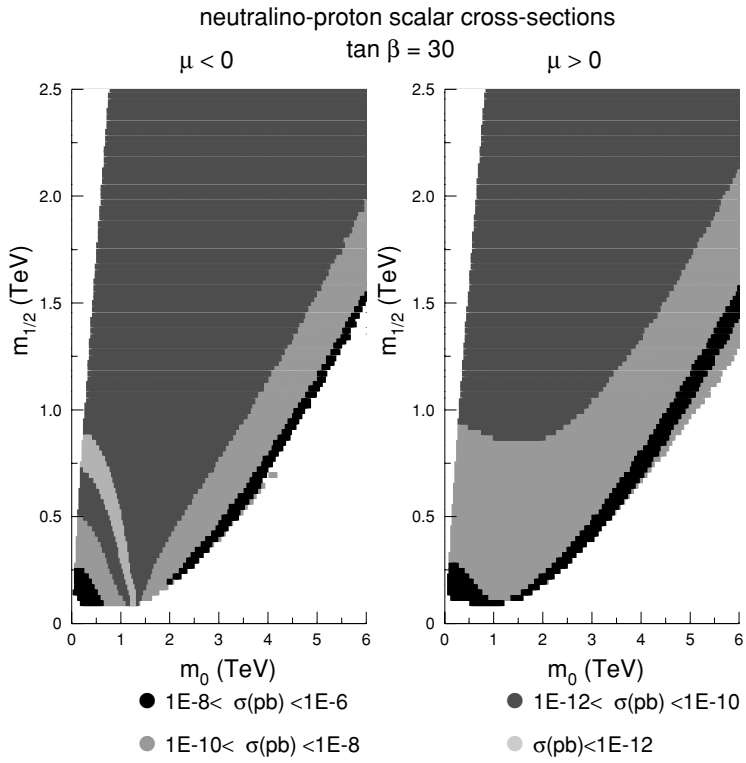

Figure 9.15 Regions of scalar neutralino–proton cross sections in the mSUGRA model, in units of pb. The blank regions are excluded by theoretical and experimental considerations. We thank J. O'Farrill for supplying this figure.

convolution with nuclear spin form factors must be performed. Neutralino–quark and neutralino–gluon interactions (via loop diagrams) can also resolve into scalar and tensor components. These interactions can then be converted into an effective scalar neutralino–nucleon interaction involving quark and gluon parton distribution functions. The neutralino–nucleus scattering cross section can be obtained by convoluting with suitable scalar nuclear form factors. The final neutralino detection rate is obtained by multiplying by the *local* neutralino relic density (estimates are obtained from galaxy formation modeling), and appropriate functions involving the velocity distribution of relic neutralinos and the Earth's velocity around the Sun and around the galactic center. When the Earth's velocity around the Sun is aligned with the Sun's galactic velocity, the scattering rate should increase, leading to a seasonal modulation of these direct detection rates.

In Fig. 9.15, we show regions of scalar neutralino–nucleus cross section in the mSUGRA model for $\tan\beta = 30$, $A_0 = 0$, and (*a*) $\mu < 0$ or (*b*) $\mu > 0$. The left-hand side of the plots is excluded because $\tilde{\tau}_1$ becomes the LSP, and the lower right side of

https://doi.org/10.1017/9781009289801.010 Published online by Cambridge University Press

the plots is excluded due to a lack of REWSB. In frame *a*), there are regions at low m_0 and low $m_{1/2}$, and also along the HB/FP region, where direct detection cross sections exceed 10^{-9} pb. These cross sections are large enough to allow possible discovery of neutralino dark matter by Stage 3 dark matter detectors, such as Zeplin-4, Cryoarray, and, XENON. There is also a region in frame (*a*) at $m_{1/2} \sim 0.3$–0.8 TeV and $m_0 \sim 0.2$–1.2 TeV, where there is a destructive interference in the scattering cross section, and rates plunge below 10^{-12} pb. In frame (*b*), for $\mu > 0$, there are again sufficient rates for direct detection of dark matter at Stage 3 detectors in the low m_0 and low $m_{1/2}$ region, and also in the HB/FP region. This time, however, there is no destructive interference in the direct detection cross section.

9.6.3 Indirect detection of neutralinos

We have already noted that if dark matter neutralinos exist, then they should condense to form a galactic halo. In addition, relic neutralinos may collect and become gravitationally bound to the center of the Galaxy, the center of the Sun and the center of the Earth. If this happens, then a variety of *indirect* dark matter detection opportunities arise.

One possibility is that relic neutralinos may interact with nuclei in the Sun, scatter to velocities below the escape velocity, and become gravitationally bound in the solar core. The high density of neutralinos in the solar core may allow a high rate for neutralino annihilation into SM particles. (Neutralinos may also collect in the core of the Earth and experience enhanced annihilation, but rates are typically smaller than from the Sun.) Most SM annihilation products will be immediately absorbed by the solar material. However, high energy neutrinos arising from neutralino annihilation may escape the Sun, and be detected by neutrino telescopes such as Antares (a water Cherenkov device in the Mediterranean) or IceCube (an array of phototubes deployed in the ice at the South Pole). Muon neutrinos would convert to muons in the water or ice, and Cherenkov radiation from the muons could be detected. The rate for neutralino annihilation in the solar core is given by

$$\Gamma = \frac{1}{2} C \tanh^2(\sqrt{CA}t_\odot), \tag{9.35}$$

where C is the solar capture rate, A is the total annihilation rate times relative velocity per unit volume, and $t_\odot$ is the present age of the Sun. For the Sun, the age of the Solar System exceeds the equilibration time, so $\Gamma \sim C/2$. Thus, highest rates for neutrinos from solar core annihilations occur in parameter space regions where the neutralino–nucleus scattering cross section is largest. From Fig. 9.15, this would mean the bulk annihilation region or the HB/FP region. It is intriguing that these regions also have low relic densities in accord with the WMAP analysis.

https://doi.org/10.1017/9781009289801.010 Published online by Cambridge University Press

Another possibility for indirect neutralino dark matter detection occurs if neutralinos annihilate in the galactic core or halo to SM particles. High energy photons can be produced as part of the annihilation products, and can be detected by gamma ray observatories. In this case, the highest rates for gamma ray detection occur in regions of parameter space where the neutralino annihilation cross section times velocity is largest: i.e. in the bulk annihilation region, the HB/FP region or in the A-annihilation funnel. Since the neutralino density is expected to be high around the galactic core, a directional signal may be found emanating from this source. Neutralinos may also annihilate via loop diagrams as $\widetilde{Z}_1\widetilde{Z}_1 \to \gamma\gamma$. In this case, the rate would be quite low, but the signature spectacular, since the gamma ray energy would be essentially equal to $m_{\widetilde{Z}_1}$.

Finally, neutralinos present in the galactic halo may also annihilate, leading to positrons or antiprotons, which may be detected by cosmic ray detectors. In this case, the e^+s or $\bar{p}$s would likely be non-directional, since their path of flight would be bent by galactic magnetic fields. Again, the highest rates are to be expected where the neutralino annihilation cross section is highest: in the bulk region, the HB/FP region or the A-annihilation funnel. The rates for detection of the indirect signals depend on assumptions regarding the density profile of neutralinos in the galactic core and halo. Clearly, if clumping of dark matter occurs, then rates may be higher than expected. Alternatively, if the galactic halo neutralino density profile has been overestimated, then signal rates may be lower than expected.

In principle, the results of direct and indirect dark matter searches may pinpoint the mechanism responsible for depletion of neutralinos in the early Universe so that the current value of the relic density is consistent with WMAP results. The bulk annihilation region at low m_0 and low $m_{1/2}$ may give rise to large signal rates in *all* direct and indirect search experiments. However, this region is largely disallowed due to large contributions to $(g-2)_\mu$, $BF(b \to s\gamma)$ and a value of m_h lower than bounds from LEP2. The stau co-annihilation region is likely to give *no* signals for neutralino direct or indirect detection, while *all* signals for direct and indirect neutralino detection may be possible in the HB/FP region. If neutralino annihilation through the broad A and H resonances is the main sink for neutralinos in the early Universe, then direct neutralino detection and also detection of neutrinos from neutralino annihilation in the core of the Sun are unlikely. However, detection of γs, e^+s, and $\bar{p}$s from neutralino annihilation in the galactic core and halo may occur at detectable rates.

9.7 Neutrino masses

Data from solar and atmospheric neutrino experiments provide unambiguous evidence for neutrino oscillations, and strongly suggest an interpretation in terms of

https://doi.org/10.1017/9781009289801.010 Published online by Cambridge University Press

neutrino masses and mixings. These data are consistent with a hierarchical structure of neutrino masses, with $m_{\nu_e} \ll m_{\nu_\mu} \ll m_{\nu_\tau}$ and $m_{\nu_\tau} \sim 0.05$ eV and near-maximal neutrino mixing, though other mass patterns are certainly possible. Cosmological data also tell us that neutrinos are all lighter than a few eV.

We have seen, however, that like the SM, the MSSM (which after all is essentally a direct supersymmetrization of the SM) does not allow for neutrino masses. As in the SM, one can allow for lepton number conserving Dirac neutrino masses by introducing neutrino Yukawa couplings into the superpotential. This necessarily entails the introduction of new right-handed neutrino (RHN) superfields. Since neutrinos are electrically neutral, it is also possible to introduce lepton number violating Majorana mass terms for these. Within the SM, the well-known see-saw mechanism provides an elegant way of obtaining the small values of neutrino masses indicated by the data;[30] in the supersymmetric context, this again requires the introduction of RHN superfields. Within the supersymmetric framework, Majorana masses for neutrinos are also obtained if the superpotential includes lepton number and R-parity violating interactions, *without* the need for any new RHN superfields. This is discussed in detail in Chapter 16. Here, we will confine our attention to the simplest extension of the MSSM that accommodates the incorporation of neutrino masses via the see-saw mechanism. This, of course, requires us to extend the superfield content of the MSSM by the RHN superfields, one for each generation.

9.7.1 The MSSM plus right-handed neutrinos

In order to implement the see-saw mechanism for neutrino masses, we are led to introduce three additional gauge singlet left-chiral scalar superfields $\hat{N}_i^c$ ($i = 1$–3 denotes the generation),

$$\hat{N}_i^c = \tilde{\nu}_{\mathrm{R}i}^\dagger(\hat{x}) + \mathrm{i}\sqrt{2}\bar{\theta}\psi_{N_i^c\mathrm{L}}(\hat{x}) + \mathrm{i}\bar{\theta}\theta_{\mathrm{L}}\mathcal{F}_{N_i^c}(\hat{x}),$$

whose Majorana fermion component destroys left-handed $SU(2)$ singlet anti-neutrinos, or create the corresponding right-handed neutrinos ($\nu_{\mathrm{R}i}$). These singlet superfields are coupled to other MSSM superfields via the superpotential

$$\hat{f} = \hat{f}_{\mathrm{MSSM}} + (\mathbf{f}_\nu)_{ij}\epsilon_{ab}\hat{L}_i^a\hat{H}_u^b\hat{N}_j^c + \frac{1}{2}M_{Ni}\hat{N}_i^c\hat{N}_i^c, \tag{9.36}$$

[30] The see-saw mechanism has an interesting history. To our knowledge, the see-saw formula for the neutrino mass first appears in H. Fritzsch and P. Minkowski, *Phys. Lett.* **B62**, 72 (1976) and P. Minkowski, *Phys. Lett.* **B67**, 421 (1977). The mechanism was independently invented and cast into its modern form by T. Yanagida, KEK Report No. 79-18 (1979); M. Gell-Mann, P. Ramond and R. Slansky, in *Supergravity*, D. Freedman *et al.*, Editors, North-Holland, Amsterdam (1980); S. Glashow, in *Quarks and Leptons, Cargèse 1979*, M. Lévy *et al.*, Editors, Plenum (1980); R. Mohapatra and G. Senjanovic, *Phys. Rev. Lett.* **44**, 912 (1980). For a recent review of the original idea and its variants, see e.g. R. Mohapatra, hep-ph/9910365.

https://doi.org/10.1017/9781009289801.010 Published online by Cambridge University Press

where summation over generation indices i and j as well as $SU(2)$ indices a and b is implied. Notice that the superpotential includes lepton number violating Majorana mass parameters M_{Ni} for these right-handed neutrinos. In (9.36) we have, without loss of generality, chosen a basis for the RHN superfields so that the superpotential mass terms are diagonal. Since the mass terms for these gauge singlet superfields are not forbidden by symmetry considerations (other than ad hoc global symmetries such as lepton number conservation), these are naturally expected to be large – $\sim M_{\rm Planck}$ in the present framework, or comparable to the $SO(10)$ breaking scale if the model is embedded into an $SO(10)$ GUT, as discussed in Chapter 11. Indeed, values of M_{Ni} well beyond the weak scale and ranging up to $M_{\rm GUT}$ are favored by SUSY GUT models which seek to explain neutrino oscillation data. When electroweak symmetry is broken, Dirac neutrino mass entries $(m_D)_{ij}$ are also induced. The resulting 6×6 neutrino mass matrix must be diagonalized to obtain the masses of the physical neutrinos. Assuming that $(m_D)_{ij} \ll M_i$ for all i and j, we know that there must be three nearly sterile, heavy Majorana neutrinos with masses very close to M_i. Since these essentially saturate the trace, there must be three light active Majorana neutrinos with masses that depend on the details of the Dirac mass matrix, but whose values vary inversely as the M_i. In the limit where we ignore the mixing of active neutrino flavors (not a good approximation to the data), the formulae become simple and we have $m_{\nu_i} \simeq m_{Di}^2/M_{Ni}$ as the mass of the active neutrino of generation i. Though the neutrino masses would be different in the case of mixed neutrinos, we would expect that this simple formula reproduces their order of magnitude.

The soft SUSY breaking terms must now also be augmented to include

$$\mathcal{L} \ni \mathcal{L}_{\rm MSSM} - \tilde{\nu}_{{\rm R}i}^\dagger \mathbf{m}_{\tilde{\nu}_{\rm R}}{}^2_{ij} \tilde{\nu}_{{\rm R}j} + \left[(\mathbf{a}_\nu)_{ij} \epsilon_{ab} \tilde{L}_i^a \tilde{H}_u^b \tilde{\nu}_{{\rm R}j}^\dagger + \frac{1}{2} b_{\nu ij} \tilde{\nu}_{{\rm R}i} \tilde{\nu}_{{\rm R}j} + \quad \text{h.c.} \right], \tag{9.37}$$

where once again a summation over repeated indices is implied. The parameters $(\mathbf{m}_{\tilde{\nu}_{\rm R}})_{ij}$, $(\mathbf{a}_\nu)_{ij}$, and $b_{\nu ij}$ are assumed to be of order the weak scale. Assuming that $M_i \gg M_W$, the right-handed sneutrinos have masses $\sim M_{Ni}$ and, like the $\nu_{{\rm R}i}$'s, decouple from the low energy theory. When considering the renormalization group evolution of couplings and SSB parameters, one must remember that for energy scales above $Q = M_{Ni}$, the effective theory is the MSSM augmented by the corresponding right-handed neutrinos and sneutrinos, while at scales below the smallest of the M_{Ni}, these are all integrated out, leaving the MSSM as the effective field theory. Indeed, the RGEs of the MSSM must be augmented to include potentially significant effects of the new neutrino Yukawa couplings.[31]

[31] The RGEs for the MSSM augmented by a RHN are listed, for instance, in H. Baer *et al.*, *JHEP* **04**, 016 (2000).

https://doi.org/10.1017/9781009289801.010 Published online by Cambridge University Press

The inclusion of the new neutrino-sector superpotential and soft SUSY breaking parameters can in general lead to lepton-flavor-violating processes (LFV).[32] Even in the case where one assumes mSUGRA-like conditions at $Q = M_{\rm GUT}$ on the new parameters, neutrino Yukawa coupling contributions to renormalization group evolution between $M_{\rm GUT}$ and M_{Ni} can induce off-diagonal slepton mass matrix entries that lead to LFV processes like $\mu \to e\gamma$, $\mu \to e$ conversion, $\tau \to \mu\gamma$ or $\mu^- \to e^+e^-e^-$ at potentially observable rates. The stringent experimental limits on these rare decays strongly constrain the neutrino sector parameters. In the future, discovery of LFV processes may help pin down the parameters associated with the right-handed neutrinos. Of course, LFV could also show up in the direct decays of sparticles, for instance $\widetilde{Z}_j \to \ell_1^+\ell_2^-\widetilde{Z}_i$ or $\tilde{\ell}_1 \to \ell_2\widetilde{Z}_i$, if these are produced at future colliders. We should also mention that renormalization effects from neutrino Yukawa couplings would cause small inter-generation splitting between the sneutrinos, in much the same way that the tau Yukawa interaction splits $m_{\tilde{e}_{\rm L}}$ from $m_{\tilde{\tau}_{\rm L}}$. These splittings may provide a direct test of the see-saw mechanism if sneutrino masses are precisely measured in the future.

Finally, we mention that the existence of long-lived, heavy right-handed Majorana neutrinos and sneutrinos offers a novel solution of the baryogenesis problem via leptogenesis, provided that neutrino Yukawa interactions also violate CP conservation. This is possible in the same way that SM quark interactions do not conserve CP. Assuming that CP is violated, there will be a difference in the rates for the decay of $\nu_{\rm R}$ into leptons and antileptons at the one-loop level, so that a leptonic matter–antimatter asymmetry can be induced at temperature $T \lesssim M_{Ni}$, below which the right-handed neutrinos and sneutrinos fall out of thermal equilibrium. This lepton asymmetry is then converted to a baryon asymmetry at lower temperatures via sphaleron interactions, as discussed in Chapter 16.[33]

[32] For an overview, see Y. Kuno and Y. Okada, *Rev. Mod. Phys.* **73**, 151 (2001).
[33] See M. Fukugita and T. Yanagida, *Phys. Lett.* **B174**, 45 (1986).

https://doi.org/10.1017/9781009289801.010 Published online by Cambridge University Press